REACTIONS OF THE {100} FACE OF GALLIUM ARSENIDE WITH MOLECULAR AND ATOMIC BROMINE

By

IAN McKENZIE SALUSBURY

B.Sc. (Hons.), University of Bath, 1988

A THESIS SUBMITTED IN PARTIAL FULFILLMENT OF THE REQUIREMENTS FOR THE DEGREE OF MASTER OF SCIENCE

in

THE FACULTY OF GRADUATE STUDIES

Department of Chemistry

We accept this thesis as conforming to the required standard

THE UNIVERSITY OF BRITISH COLUMBIA

July 1990

In presenting this thesis in partial fulfilment of the requirements for an advanced degree at the University of British Columbia, I agree that the Library shall make it freely available for reference and study. I further agree that permission for extensive copying of this thesis for scholarly purposes may be granted by the head of my department or by his or her representatives. It is understood that copying or publication of this thesis for financial gain shall not be allowed without my written permission.

Department of CHEMISTRY

The University of British Columbia
Vancouver, Canada

Date JULY 24th 1990

Abstract

The reaction of gallium arsenide {100} with molecular and atomic bromine was studied at temperatures between 100 and 225°C and at pressures of bromine between 0.1 and 40 Torr. Samples of GaAs were placed on a silicon platform within a Pyrex reactor flow system and the etch rate was determined by profilometry or weight change of the sample. Atomic bromine was produced by a 2450 MHz microwave discharge and the samples were etched downstream. The atomic concentration was measured by an isothermal calorimetric detector.

Pressure dependence studies for molecular Br_2 etching showed that below 1-2 Torr of bromine, a first order reaction was rate-limiting whereas above this pressure a half order reaction was rate-limiting. Temperature dependence studies for the low pressure and high pressure regimes gave activation energies and pre-exponential values for the two respective rate controlling reactions. The first order reaction was found to have an activation energy of 29.2 ± 4.0 kJ mol^{-1} and a pre-exponential value of (3.4 ± 4.4) x 10^{21} molecule cm^{-2} s^{-1} $Torr^{-1}$. The activation energy for the half order reaction was found to be 8.4 ± 0.7 kJ mol^{-1} with a pre-exponential of (6.4 ± 1.3) x 10^{18} molecule cm^{-2} s^{-1} $Torr^{-1/2}$.

The activation energy for atomic etching was calculated to be 12.9 ± 0.9 kJ mol^{-1} and the pre-exponential, (7.1 ± 2.0) x 10^{20} atom cm^{-2} s^{-1} $Torr^{-1}$.

Table of Contents

List of Tables

List of Figures

Acknowledgments

I would like to thank Professor E. A. Ogryzlo for his guidance and encouragement throughout the course of this work.

I am grateful to Professor D. Chong for making his linear least squares computer program available for our group's use.

My thanks also go to the Electrical and Mechanical shops for their assistance and to the glass blowers, Steve and Sean, for their help and patience.

The kinetic analysis given in the discussion section was first developed by Z. H. Walker and my thanks go to him for its use.

The advice and encouragement of Mark, Paul and Zane in the lab is gratefully acknowledged. They helped to make my time at U.B.C. as enjoyable as it has been.

Finally, I would like to express my gratitude to my family and friends for their support and interest over the last two years.

1 INTRODUCTION

1.1 HISTORICAL PERSPECTIVE

The invention of the bipolar transistor by J. Bardeen, W. H. Brattain and W. Shockley of the Bell Telephone Laboratories, in 1948, was the beginning of a second industrial revolution.[1] Microelectronic technology has provided the driving force behind the rapid post-war advances in science, engineering and the information industry.

The properties of semiconductors such as silver sulphide, have been investigated since the last century and in the early days of radio the detector in all receivers was the crystal rectifier, usually a galena crystal.[2] This situation changed with the introduction of cheap thermionic (or vacuum) tubes in the early twentieth century and almost all electronic equipment became based on vacuum tubes. They were used as switches or amplifiers to magnify electrical signals but their size, lack of reliability and high power dissipation restricted their usefulness.[3]

The first transistor was made from germanium because of the ease of growing good single crystals. However, germanium was affected by operating temperature limitations due to its relatively small bandgap and so alternative materials were sought. The larger band gap and superior oxide of silicon prompted research into its use and by 1952, the preparation of single crystals of silicon had been reported[4], with the first silicon transistors becoming commercially available two years later.

The transistor provided low power, small and robust electronic switches and amplifiers and quickly replaced the vacuum tube. The

demand from the computer industry was a major driving force for transistor production. The next stage in microelectronic development was the production of the integrated circuit (IC), the first of which became commercially available in 1960. A monolithic integrated circuit or chip is defined as the "microstructure of many circuit elements inseparably associated on or within a continuous substrate"[5]. Instead of the assembly of components one by one and the consequent complex wiring, only a series of photographic processes determines the locations of several million components on a wafer. The advantages of integration are reflected by the change in the maximum number of components per chip since 1960. At that time one or two devices were put on each chip and that has now risen to 16 million devices per chip, with over 30,000 components mm^{-2}. This level of integration is known as Very Large Scale Integration (VLSI). The levels of integration are loosely defined by these figures : 100 components for standard integrated circuits, 10,000 components for standard LSI and 1 million components for standard VLSI. The next stage in development has been named ultra large scale integration (ULSI).[6]

The predominance of silicon in microelectronic device fabrication is due to a number of factors. Si has a suitably high band-gap (1.1eV) so that it can operate throughout a reasonable temperature range. Silicon can be used at temperatures up to 200°C, which compares to a maximum of 75°C for germanium.[7] Also Si is the second most abundant element in the Earth's crust and so is inexpensive and in an inexhaustible supply. The material properties of Si enable large single crystals, essentially dislocation free, to be grown and then annealed, sawn and polished with well established techniques. Finally, Si forms a stable oxide when exposed to oxidising agents at high temperatures, which can be utilised as

a dielectric layer or a protective mask. Desired electronic properties can be produced by inserting impurities (by diffusion or ion implantation) into selected areas of the wafer surface, from which oxide has been stripped.

Despite silicon's long established technology and many capabilities, the variety of tasks for which semiconductors are required demands a variety of semiconductors to perform them. For example, germanium is still used in high voltage transistors. The potential for using III-V compounds (that is compounds formed between elements of Groups IIIA and VA of the periodic table) was realised in the early stages of microelectronics research. During the 1950's there was a considerable research effort in this field[8], however because of the physical properties of the materials and processing problems it is only within the last decade that these materials have found commercial use. They enjoy processing speeds unequalled by silicon and have many optoelectronic applications. The most important examples are gallium arsenide (GaAs) and indium phosphide (InP).

1.2 CRYSTAL STRUCTURE OF GALLIUM ARSENIDE

Gallium arsenide crystallises in the zincblende (or sphalerite) structure. This structure consists of two interpenetrating face centred cubic lattices with one of the sublattices displaced one quarter of the way along the main diagonal of the other. Figure 1.1 shows this configuration : one sublattice consists of gallium atoms and the other arsenic atoms[9]. The bonding is polar covalent (32% ionic character)[10] with the charge concentrated on the As atoms. Hereafter, { }, ( ) and [ ] will refer to families of planes, specific planes and directions of planes, respectively. The most significant feature of the GaAs structure is that the structure is

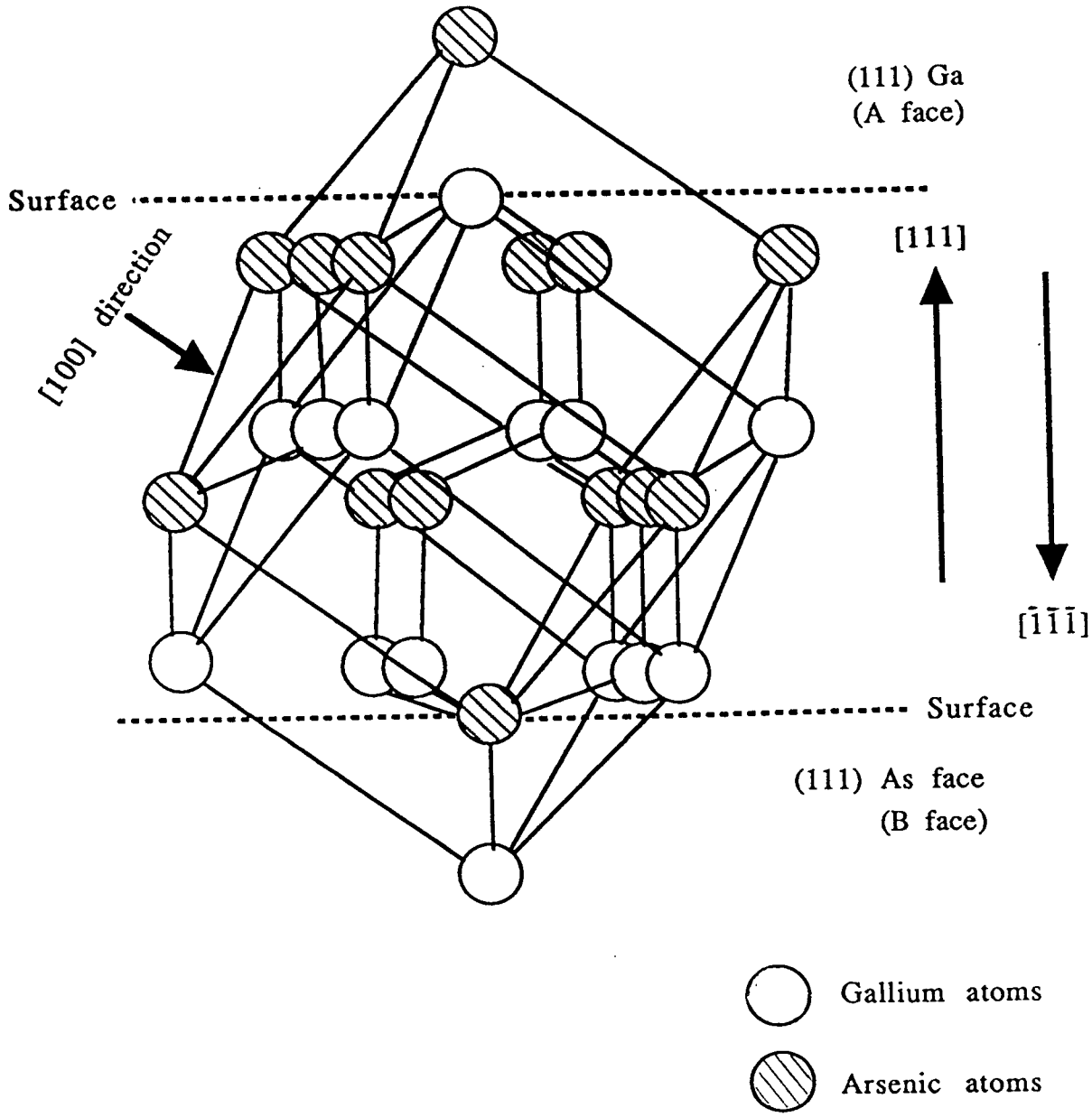

Figure 1.1 The zincblende lattice observed perpendicular to a [111] axis and along a [110] axis.

asymmetric ; the [111] axis is polar. The $(\bar{1}\bar{1}\bar{1})$ plane in the figure is called the Ga (111) face or A face and the (111) plane is the As (111) face or B face. If we consider the Ga (111) face we can see that two possible surface states exist. An As atom could be connected to one Ga atom below, leaving the As atom with three 'dangling' bonds, that is three unpaired electrons. However, this state appears too energetically unfavourable to be found as a surface state in a cleaved crystal. Alternatively, there can be a Ga atom attached by three bonds to arsenic atoms in the layer below, so that the Ga has one bond coming out of the plane. Therefore, if the Ga atoms in this face are neutral, they have no free electrons as their three valence electrons are used for bonding. If we now consider the As (111) face, we can see that the favoured state involves As atoms connected to three Ga atoms, leaving one non-bonding pair of electrons if the atom is neutral. So each As atom has two free electrons since only three of their five valence electrons are used in bonding (figs 1.2a and 1.2b). Thus the As {111} faces are more readily etched and at temperatures below 770°C, evaporation takes place more rapidly from their surface. Also oxidation of As {111} planes occurs more quickly.

The {100} planes consist of either all Ga or As atoms (fig. 1.2c). The [100] direction is not polar and so all {100} planes behave identically. {100} planes are found to etch more slowly than As {111} planes and faster than Ga {111} planes.[11] This disparity in etch rates causes the phenomenon of crystallographic etching. For example, when the {100} plane is etched with an appropriately aligned striped mask in place, V-shaped (fig. 1.3a) or reverse mesa shaped grooves form (fig. 1.3b)[12]. This feature has been utilised in the fabrication of VMOS (vertical metal-oxide-semiconductor) devices.

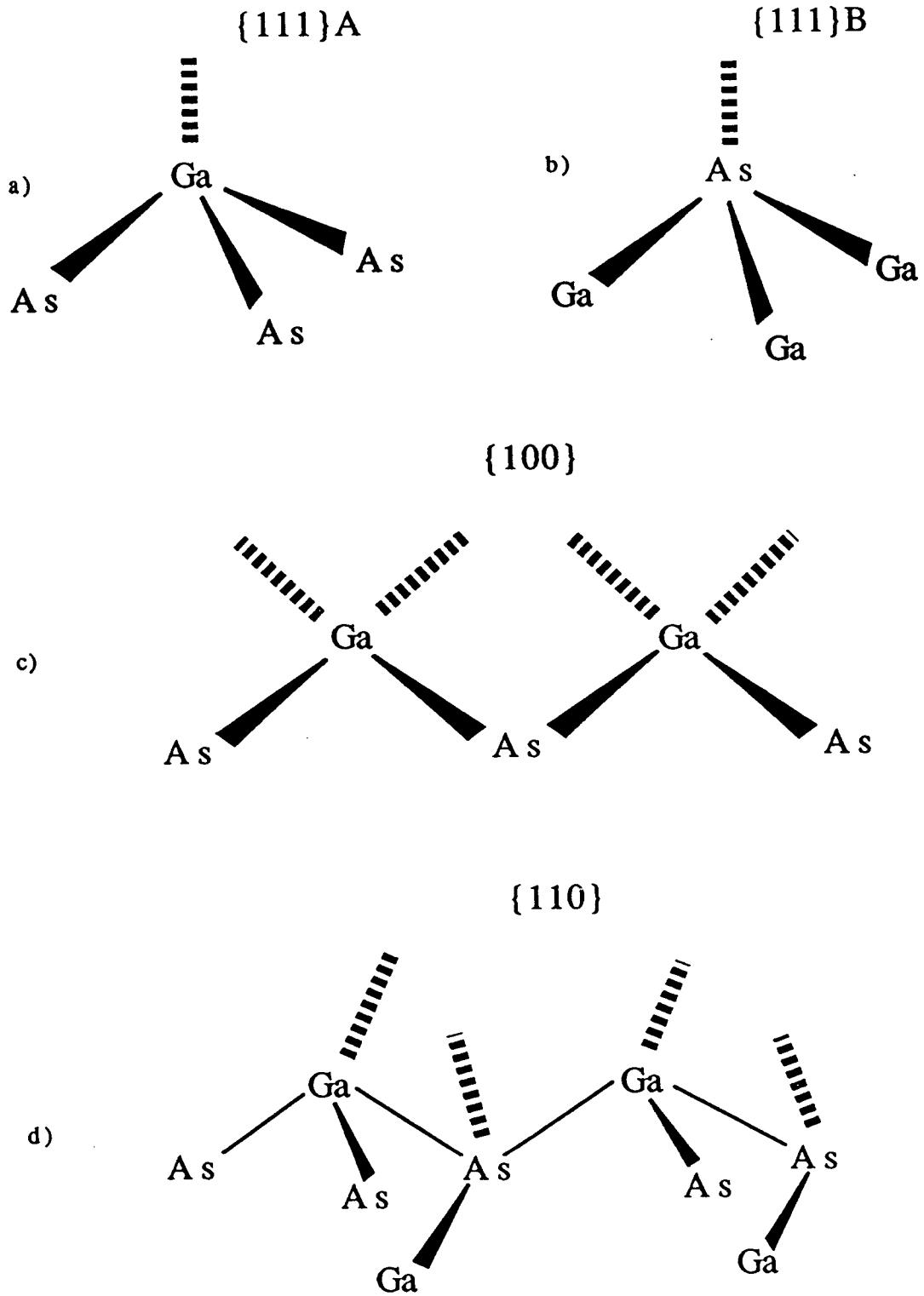

Figure 1.2 Schematic representation of the surface bonding on the {111}, {100} and {110} planes of GaAs

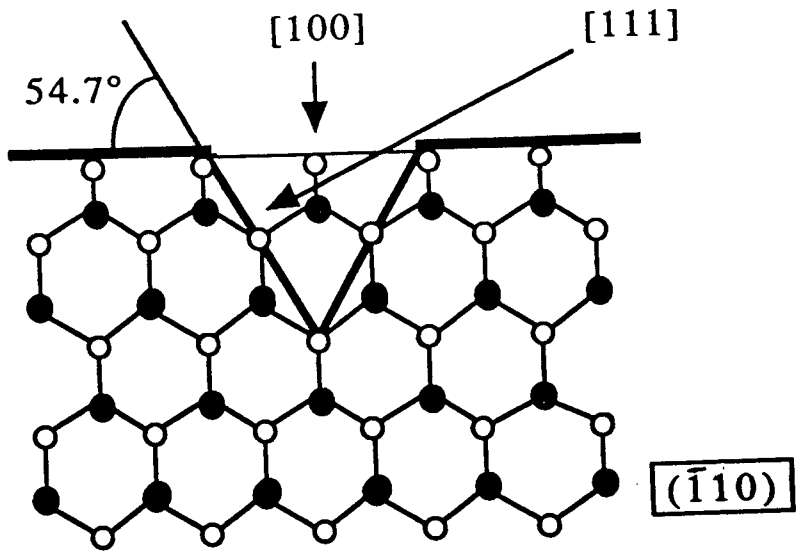

(a)

○ Gallium atom
● Arsenic atom

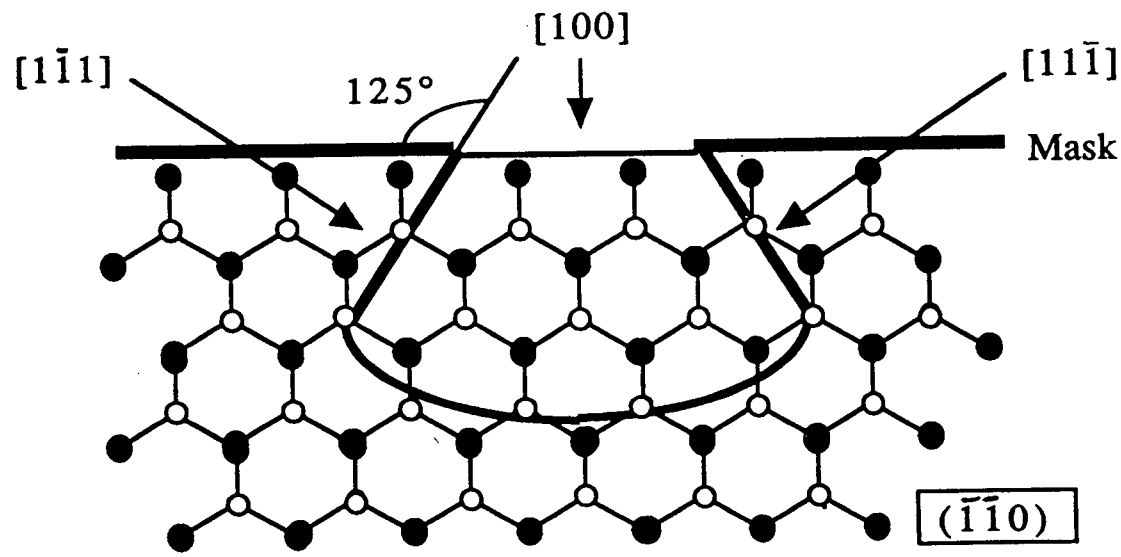

(b)

Figure 1.3 Crystallographic etching of {100} GaAs, which results in (a) V-shaped groove or (b) reverse mesa formation

The {110} cleavage planes intersect the {100} planes at right angles and in the {110} face an equal number of Ga and As atoms occur (fig. 1.2d). Each Ga atom is bound to two As atoms in the plane and a third bond is directed into the interior of the crystal.

1.3 GALLIUM ARSENIDE IN ELECTRONIC DEVICES

The development of GaAs integrated circuits was dependent on the production of high quality substrates and this proved problematic. Some methods used in producing and then treating silicon crystals are sometimes not viable for compounds. For example, in the Czochralski technique for crystal growth a seed crystal is slowly withdrawn from a 'melt'. It has proven difficult to prevent decomposition of a GaAs melt since the arsenic component is more volatile than the gallium. Similarly, annealing processes to remove defects cause selective vaporisation of arsenic. New techniques such as liquid encapsulated Czochralski (LEC) have been developed to prevent the vaporisation of arsenic.[13]

GaAs is also more brittle than Si and so is more difficult to process. These combined problems mean that it is still not possible to produce GaAs wafers that are as large as Si wafers.

In contrast to Si, the native oxides of Ga and As are not suitable as dielectrics or passivating layers. Therefore, other means must be devised to form insulating structures.

GaAs has many useful properties, which make these problems worth overcoming (Table 1.1).[14] GaAs has a higher electron mobility and drift velocity than Si and so the switching speed is faster. The fastest switching speed reported for any transistor is 250 x 10^9 switches per second, which was achieved by a transistor made of layers of aluminium indium arsenide and gallium indium arsenide on an indium phosphide

Table 1.1 Physical properties of silicon and gallium arsenide

	Silicon	Gallium Arsenide
Crystal structure	Diamond	Zincblende
Lattice constant (Å)	5.43	5.64
Atomic/molecular wt	28.09	144.63
Density (g cm^{-3})	2.33	5.32
Band gap (eV)	1.12	1.42
Type of band gap	Indirect	Direct
Drift mobility (cm^2 V^{-1} s^{-1})		
Electrons	1500	8500
Holes	450	400

base. In contrast, the fastest reported switching speed for a silicon transistor is 75 x 10^9 switches per second.[15] This speed advantage has already been exploited in some mainframe and supercomputers. The Cray 3 supercomputer, the first of its kind to be based on GaAs, will have a clock speed as high as 300 megaHertz.[16]

High electron mobility is also important for high frequency, low noise operation. The lower noise operation of GaAs circuits turns out to be particularly valuable for the detection of television and microwave signals. Therefore, GaAs detectors are widely used in satellite receiving dishes. Stronger fields than 10,000 V cm^{-1} elicit additional physical interactions and GaAs loses its advantage over silicon.

Band-gap size determines the range of temperatures at which a semiconductor can operate. Therefore, GaAs integrated circuits can function at higher temperatures than Si. Also the band-gap in GaAs can be engineered by alloying with another element. For example, aluminium arsenide has a much wider band gap than GaAs. So partial substitution to form Al_xGa_{1-x} As, produces band gaps directly proportional to the mole fraction x of aluminium.

Another major advantage of GaAs and all other direct band-gap semiconductors is the optoelectronic capabilities, which the direct band-gap offers. In direct band-gap semiconductors, the conduction band minimum is located at the same momentum value as the valence band maximum. Thus an electron can more readily make a transition from the conduction band to the valence band by radiating a photon.[17] This process can also be reversed so that a photon is absorbed and converted into electrical energy. By converting light energy into electrical energy, GaAs can act as a photodetector and can be integrated into high speed GaAs electronic circuitry.

Such transitions cannot occur efficiently in indirect band-gap semiconductors without an accompanying nonradiative reaction, such as a collision, to conserve momentum.[18] Since GaAs can efficiently convert electrical energy into light it is used to make light emitting diodes (LED) and diode lasers. The wavelength of the light depends on the band-gap size. Diode lasers emit radiation at near infrared wavelengths and the output can be shifted by alloying with aluminium, indium or phosphorus, by the so-called band-gap engineering mentioned previously. Such lasers are widely used in optical fibre based communications.

1.4 PROCESSING TECHNOLOGY

Microelectronics processing involves several stages (fig. 1.4). Firstly, a crystal is grown and then annealed by heating, for elemental semiconductors, such as silicon. This minimises defects in the crystal. Then the crystal is sawn, polished and cleaned to produce wafers (up to 20 cm in diameter). Next the desired electrical properties are introduced by doping with impurities.

Pattern generation on the wafer is accomplished by laying down a photoresist. This is patterned by applying a mask and then exposing it to light. Photoresists can create negative or positive images. In the former case, bonds crosslink on exposure to light whereas in the latter, bonds are broken. The developed photoresist must then be removed by hot oxidising agents (H_2SO_4-H_2O_2), solvents or an oxygen plasma.

Once the desired structures have been etched into the wafer the resist can be removed. To produce metal oxide semiconductor integrated circuits, various metal and oxide layers must be layed down. This usually requires the repetition of the pattern generation and etching stages.

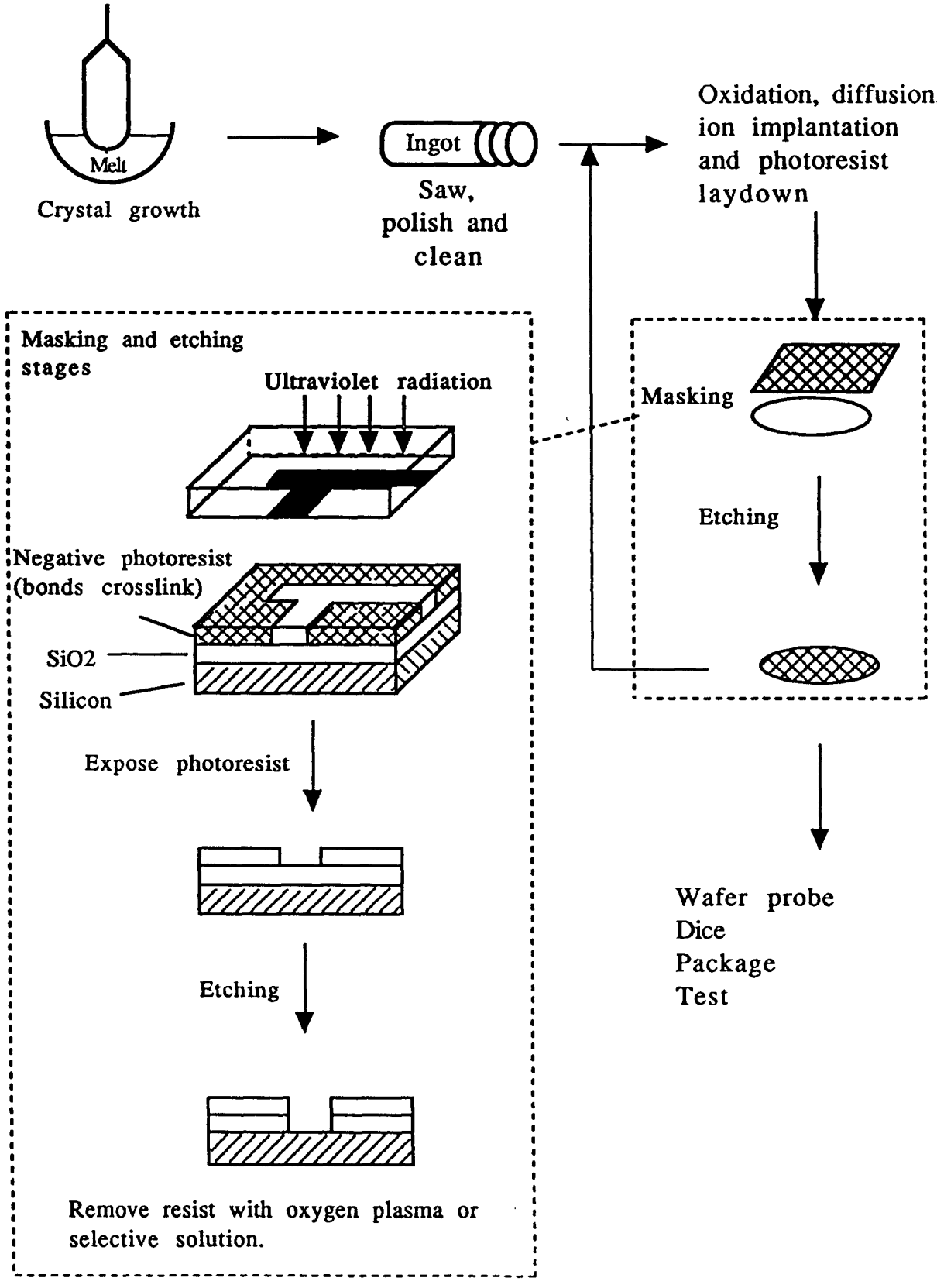

Figure 1.4 Schematic diagram of microelectronic processing

The process under consideration in this thesis is etching. Etching has many applications including patterning of semiconductor, conductor and insulating materials, stripping the ingot, cleaning and polishing the wafers.

1.5 ETCHING PROCESSES

Etching can be defined as the removal of solid material by chemical reactions or physical processes. Chemical etching processes fall into two categories : wet etching and dry etching. Wet etching is performed by simple immersion in the etchant solution. As for any chemical reaction, the rate depends on the temperature of the reactants and so temperature control is critical for attaining optimum rates. Wet etching has been the dominant etching technique in silicon technology but undercutting of the mask can occur. Ideally, an etch should be anisotropic (fig. 1.5a), which produces vertical walled etch figures, rather than isotropic, which restricts the resolution of features (fig. 1.5b). A 1% solution of bromine in methanol is a common etchant for GaAs and because of the selective etching of certain crystal faces some degree of anisotropy can be attained.

Dry etching encompasses plasma etching, ion etching, laser assisted etching and molecular gas phase etching. In ion etching processes, such as sputtering and reactive ion etching (RIE), ion bombardment plays a major role in the etching. Laser assisted etching can be performed in the liquid or gas phase and involves photochemical etching. The irradiation of a semiconductor with photons that can excite electrons above the band gap causes the production of electron-hole pairs and this may open an alternative photochemical reaction pathway to that of the thermal reaction.[19,20]

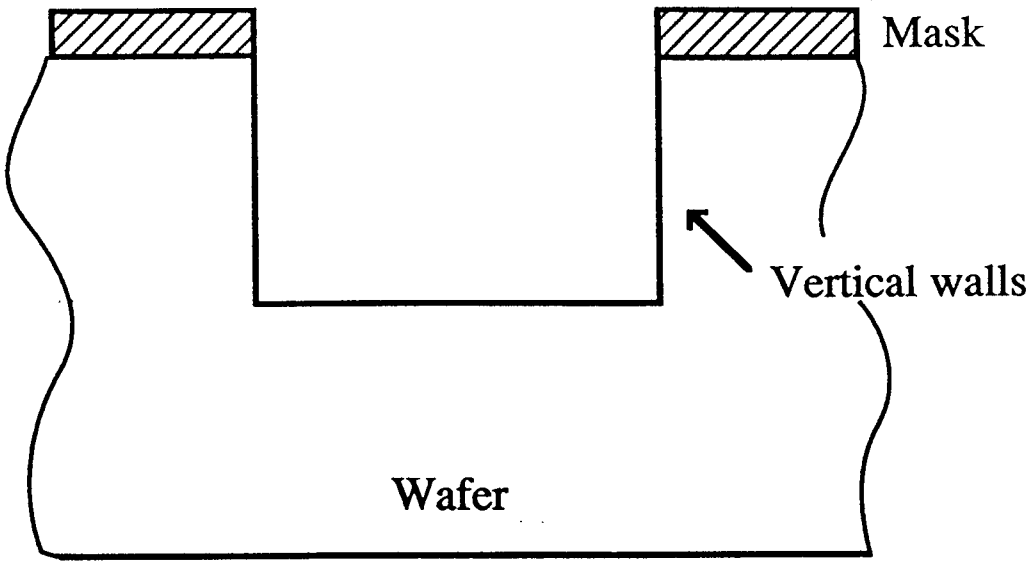

(a)

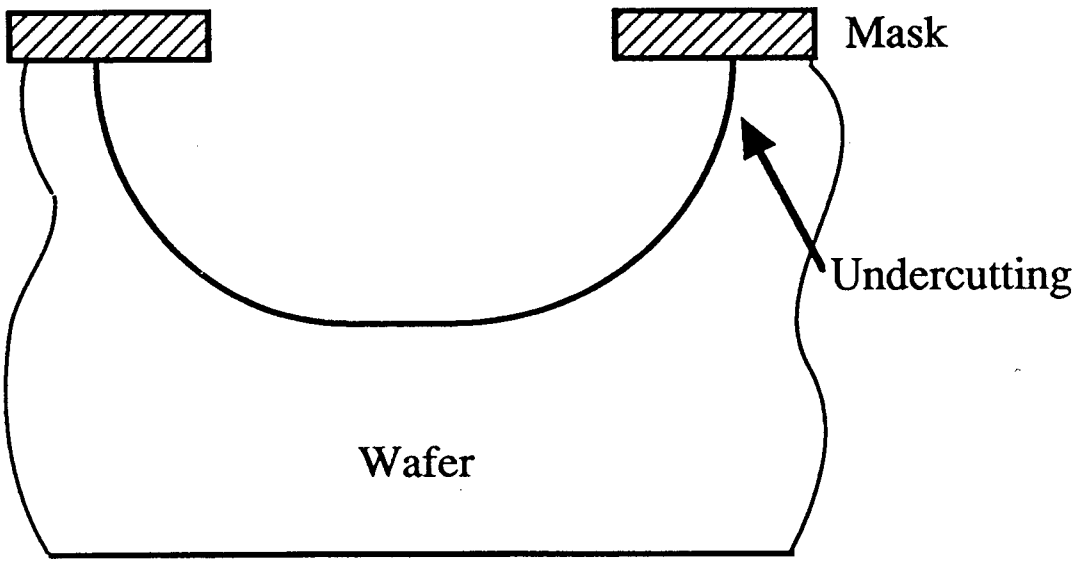

(b)

Figure 1.5 Profiles of (a) anisotropic and (b) isotropic etches

Plasma etching uses molecular gases, usually containing one or more halogen atoms. The molecules are dissociated in a radio frequency discharge at pressures between 0.01 and 10 Torr, to produce a partially ionised gas composed of ions, electrons, molecules and free radicals.[21] The temperature in plasmas, as measured by the kinetic energy of the gas molecules and ions is only 50-100°C and so a plasma can be considered as an "ensemble of highly reactive particles in a relatively cool medium".[22] After the collision of the etchant with the semiconductor surface, these species react and the products desorb and subsequently diffuse in the etch chamber. Plasma etching is carried out in barrel or planar reactors. Barrel type plasma etching is already used in LSI processing (fig. 1.6a). Wafers are loaded into a barrel shaped quartz chamber and rf power is applied to electrodes attached outside the chamber. In a planar reactor, the wafers are placed at one of the electrodes and ion bombardment results in the etch rate being greater on the axis between the electrodes (fig. 1.6b). So the anisotropy achieved in planar reactors is higher than in barrel reactors but there is also a lack of homogeneity in the etching and poorer reproducibility. Plasma etching offers a number of advantages over wet etching. Plasma processes can be highly automated as reactant or effluent can be monitored by spectrometric methods to determine the degree of etching. The highly anisotropic etches that can be achieved by the ion bombardment processes in planar reactors, facilitates the formation of sub-micron sized features.

In plasma and ion etching processes, the active species have usually been assumed to be the atomic and ionic particles. However, previous studies in this lab have shown that molecular etching often makes a significant contribution to the overall process.[23] Gas phase chemical

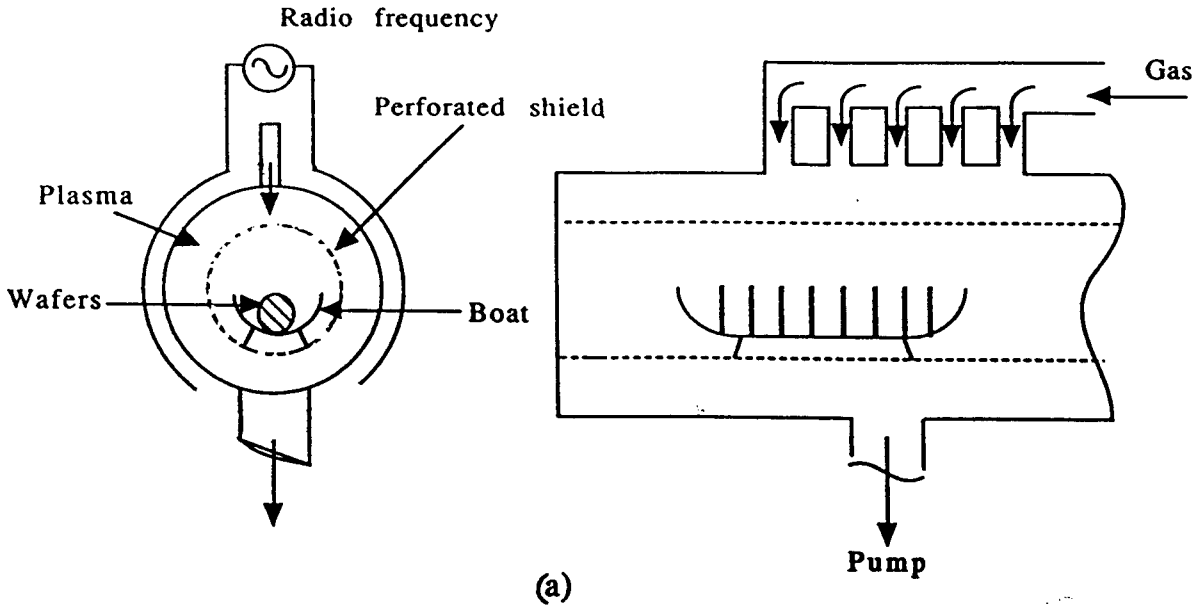

(a)

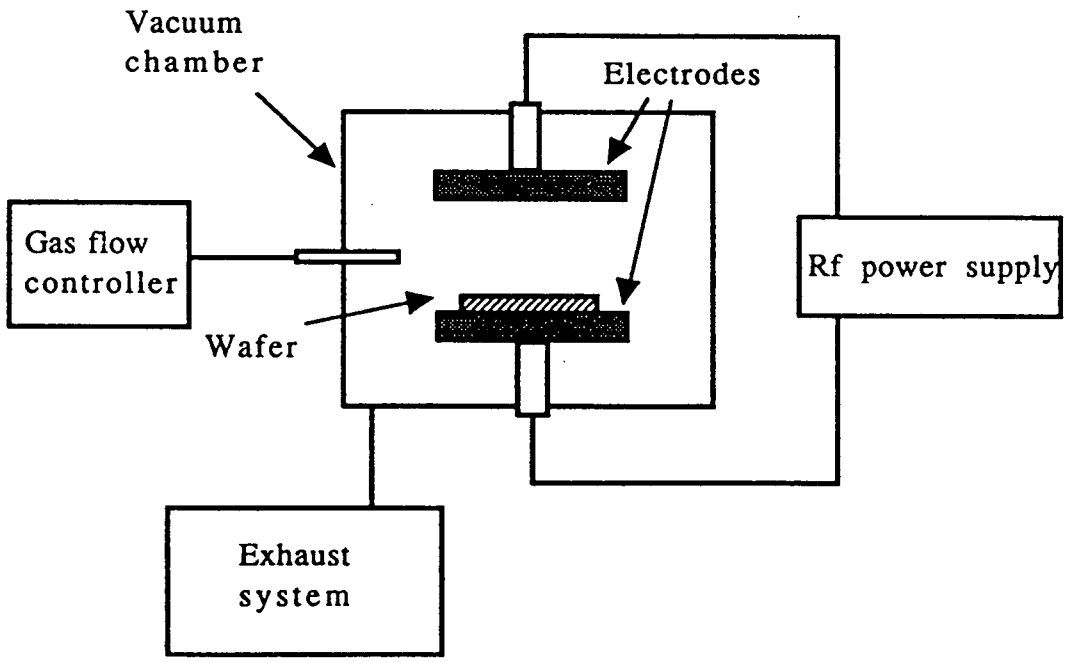

(b)

Figure 1.6 Plasma etching reactors (a) barrel (b) planar

etching is a relatively simple process involving the flow of a gas (often a halogen) at various temperatures and pressures, over a wafer. The only reactive species are the gaseous molecules. In contrast, plasma and ion etching often involve several reactive species, making the study of individual reactions difficult. Therefore, little is known about the mechanisms involved in etching in such systems.

1.6 GAS-SURFACE INTERACTIONS

Gas surface reactions can be classified into four types :

i) Heterogeneous catalysis

ii) Oxidation

iii) Chemical vapour deposition (CVD)

iv) Etching

Chemical etching shares many of the fundamental characteristics of heterogeneous catalysis, apart from the actual reaction step. In chemical etching the substrate reacts with the species from the gaseous phase rather than catalysing some reaction between gas phase molecules, which is the situation in catalysis. Therefore, most of the theories and models developed for heterogeneous catalysis can be applied to chemical etching with the minimum of adaptation. The other classes of gas-surface reactions listed differ from catalysis and etching because deposition on the surface is involved rather than the formation of gaseous products.

All gas-surface reactions involve some form of adsorption :

1.6.1 Adsorption

When a gaseous phase atom or molecule becomes bound to the surface of a solid it is said to be adsorbed. Adsorption may be physical or chemical adsorption, which are referred to by the shortened terms physisorption and chemisorption, respectively. Physisorption is the

weaker of the two interactions and involves van der Waals forces between the surface and the adsorbed molecule. The energy released is of the order of the enthalpy of condensation, usually 30 kJ mol^{-1} or less.[24] A physisorbed molecule has a residence half-life of about 10^{-8} seconds at room temperature. The time of a collision between a molecule and a surface can be considered to be of the order of a vibrational frequency (10^{-12} seconds)[25]. Therefore, physical adsorption involves the entrapment of the molecule in a shallow potential energy well for a relatively brief period. Chemisorption involves chemical bonds between adsorbed molecules and surface atoms that are comparable in strength to covalent bonds and so the heat of adsorption is usually between 200 and 500 kJ mol^{-1}.[26] However chemisorption can be much weaker than this and the distinction between physi- and chemisorption is often not easily made. Chemisorption only occurs in the first monolayer of adsorbate and once the surface is saturated, physical adsorption takes place on top of the chemisorbed monolayer.

When gaseous molecules are adsorbed they may dissociate although non-dissociative adsorption is often thought to precede the dissociation. Dissociative adsorption is seen in many catalytic processes. For example, hydrogen is adsorbed in the form of atoms on many metal surfaces and methane adsorbs dissociatively on some metals to produce CH_3 or CH_2 fragments and H atoms[27]. If adsorption is dissociative, an activation energy for the process can be observed, which is attributable to the bond length of the molecule increasing in order for chemisorption to occur. As the bonds form between the surface atoms and the adsorbed species, the heat of adsorption is evolved and the potential energy curve reaches a minimum when these bonds are at full strength. For non-dissociative adsorption an energy barrier may still have to be overcome even though

the intramolecular bonds are not broken. This barrier can arise from the reconstruction of the surface to accommodate the incoming molecules.

Typical energy profiles for adsorption are shown in fig. 1.7.[28] These are schematic diagrams and the actual potential energy curve will be a composite of the two curves shown in each diagram.

If the activation energy for chemisorption (E_c) is very slight (fig. 1.7a) the potential energy of the system may not rise above that of the free molecule and this results in rapid chemisorption. Alternatively, Ec may be large (fig. 1.7b). Therefore, to achieve chemisorption the potential energy of the system must surpass that of the free molecule and so the process will be much slower.

Generally, adsorption is found to be an exothermic process, as illustrated in fig. 1.7. However, endothermic adsorption is possible if the entropy of the system increases during the adsorption process. This is feasible if a molecule A_2 is adsorbed as two atoms since the free molecule has only three 'translational motions' and the two adsorbed A atoms each have two-dimensional movement, which is a total of four 'translational motions'.[29]

1.6.2 Models for etching reactions

Two models have been most widely used to explain gas-surface reactions : the Langmuir-Hinshelwood mechanism (1.6.2a) and the Eley-Rideal mechanism (1.6.2b). These will be discussed only as they apply to etching processes.

1.6.2a Langmuir-Hinshelwood mechanism

This mechanism comprises four fundamental steps :

(1) Transport of reactant molecules to surface.

(2)a) Non-dissociative adsorption of gas phase reactants.

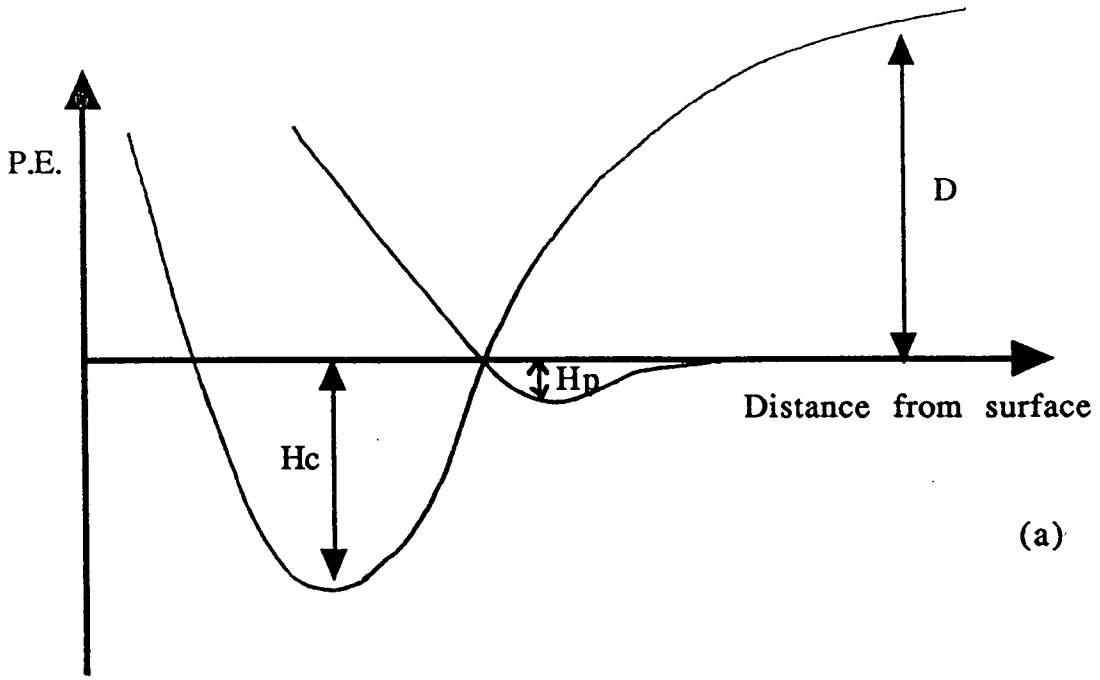

D = Dissociation energy of diatomic molecule

Hc = Heat of chemisorption

Hp = Heat of physisorption

Ec = Activation energy for chemisorption

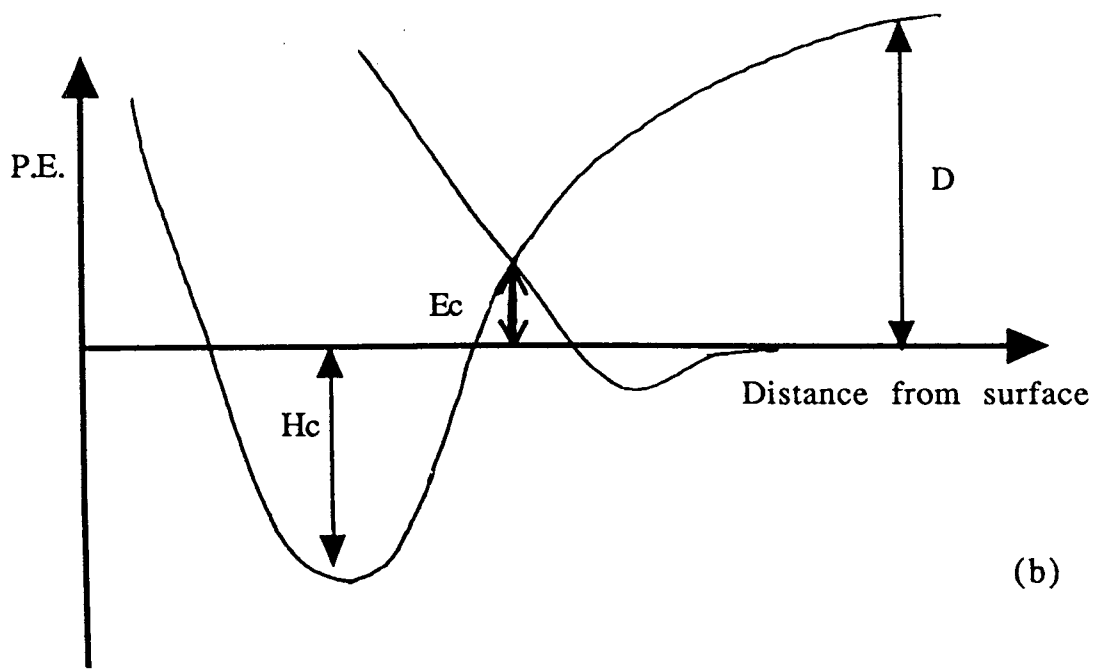

Figure 1.7 Potential energy profiles for adsorption with (a) zero Ec and (b) large Ec

and/or b) Dissociative adsorption of this adsorbed gas.

(3) Reaction between adsorbed atoms and solid surface to form adsorbed products.

(4) Desorption of the product molecules.[30]

Diffusion can be a limiting factor for porous catalysts such as zeolites or in higher pressure systems than the ones used in classical investigations. Langmuir used low pressure systems to study adsorption on tungsten filaments and the process was found to have a measurable activation energy. As diffusion in the gas phase has no activation energy, it was concluded that diffusion was not the rate limiting step in low pressure systems.[31]

1.6.2b Eley-Rideal mechanism

In this model not all the reactant molecules are strongly adsorbed since reaction was considered unlikely to occur between strongly adsorbed molecules. Therefore reaction is proposed to take place between two types of reactant molecules : a strongly adsorbed molecule, usually dissociatively adsorbed, and a molecule either from the gas phase or from a weakly adsorbed layer. This model incorporates a higher degree of mobility of the reactants than the Langmuir-Hinshelwood mechanism and has been used to account for the diffusion of hydrogen in various metals.[32]

1.7 PREVIOUS STUDIES ON GALLIUM ARSENIDE ETCHING

In III-V semiconductor etching, the volatility of the products can be rate limiting.[33] Group III fluorides are involatile at temperatures less than 300°C and so fluorine or fluorine generating plasmas create problems.[34] However, corresponding chlorides are more volatile below this temperature and there are numerous studies of chlorine-containing

plasma etching for these semiconductors. Group III and V bromides are also volatile but few studies have reported using bromine or bromine-generating plasmas. Iodine compounds are involatile.

Apart from the halogens, hydrogen and hydrogen halides are the most commonly used gases in plasma etching studies.[35] Also a variety of other etching techniques, such as reactive ion etching (RIE), laser assisted etching and molecular beam assisted etching have been applied to GaAs. Only those studies using pure halogen gases, in either atomic or molecular form, will be discussed in the following review of the literature.

Ibbotson et al[36] reported crystallographic etching of GaAs (100) with bromine and chlorine plasmas. The apparatus used was a parallel plate, radial flow reactor and concentrations of Br and Br_2 were measured by absorption spectroscopy. Reactions were carried out between 0.1 and 0.3 Torr, at a power of 0.5 W cm^{-2} and at a temperature of 100°C. Etch rates were measured from the etch depth or by monitoring the emission from elemental gallium and by etching through samples completely. It was found that the dominant reactants were Br atoms and ion bombardment did not significantly influence the etching rate. This conclusion was based on the observation that the reaction probability of bromine atoms was independent of discharge frequency. If ion bombardment enhanced the gasification reaction, this probability would increase as ion energy increased. Etching was found to be crystallographic, which is unusual in low temperature, low pressure plasmas. The relative etch rates for the planes were found to follow this order: {111}B > {100} > {110} >{111}A. Etch rates were directly proportional to Br atom concentration and ranged from 20 to 70 μm min^{-1}. With pure molecular bromine and no plasma, a much lower etch rate of 2 μm min^{-1} (at 0.3 Torr, 100°C) was measured although the etched

surface was noted to be very smooth. In a related study by the same workers the apparent activation energy for GaAs etching in a chlorine plasma was found to be 43.9 kJ mol^{-1}.[37] They proposed a general reaction scheme for III-V semiconductor etching in a chlorine plasma :

$$Cl + GaAs(surface) \longrightarrow Cl\text{-}GaAs(surf) \quad (1)$$

$$xCl\text{-}GaAs(surf) \longrightarrow AsCl_x\text{-}GaAs(surf) \quad (2)$$

$$yCl\text{-}GaAs(surf) \longrightarrow GaCl_y\text{-}GaAs(surf) \quad (3)$$

$$AsCl_x\,(ads) \longrightarrow AsCl_x(g) \quad (4)$$

$$GaCl_y\,(ads) \longrightarrow GaCl_y(g) \quad (5)$$

So at steady state, chlorine atoms adsorb on the substrate surface and react with the substrate, generating gallium and arsenic chlorides, of unknown formula. The observed etch rate for GaAs in a chlorine plasma was many orders of magnitude less than the calculated evaporation rate of gallium trichloride (20,000 μm min^{-1} at 70°C). This volatilisation was estimated from the escape of Ga_2Cl_6 molecules from a complex dimeric liquid. Assuming that the vaporisation of this dimer from a $GaCl_3$(l) layer on the GaAs surface occurs at a similar rate they excluded vaporisation as a possible rate-limiting step. If $GaCl_3$ is strongly adsorbed the formation of this dimer could be rate-limiting :

$$2GaCl_3\,(ads) \longrightarrow Ga_2Cl_6\,(ads)$$

$$Ga_2Cl_6\,(ads) \longrightarrow Ga_2Cl_6\,(g)$$

The desorption of the dimer was considered to be fast. They also proposed that the reaction of the etchant species with the GaAs surface (reactions (2) and (3) in the scheme above) may be relatively slow and so rate determining.

In the case of indium phosphide, they proposed that step (5) above was rate limiting. The activation energy for etching was very similar to the heat of sublimation of $InCl_3$ and the absolute etch rate was consistent

with the thermodynamically calculated $InCl_3(s)$ evaporation rate (45 μm min^{-1} at 250°C).

Ha[38,39] studied both molecular chlorine etching and downstream atomic chlorine of GaAs {100}. In the downstream system, the gas flows through a microwave discharge and the resulting mixture of atoms and undissociated molecules then flow over the sample. This is different than the conventional plasma etching system wherein the sample is located on or between the electrodes. Downstream etching eliminates etching due to bombardment by accelerated ions.

The etching by molecular chlorine was found to be first order at low pressures of chlorine. An activation energy of 100.3 kJ mol^{-1} was measured by determining the etch rate over the temperature range from 25-160°C. At pressures above 15 Torr the reaction appeared to reach a limiting rate with an activation energy of 57.3 kJ mol^{-1}. Atomic chlorine etching showed a first order dependence on the partial pressure of chlorine atoms and an activation energy of 37.6 kJ mol^{-1}. Both atoms and molecules displayed crystallographic etching. Reaction products, $GaCl_3$ and $AsCl_3$ were detected mass spectrometrically and provided one method of measuring the etch rate; profilometry and laser interferometry being the other methods used. A mechanism was proposed to account for the observed pressure dependencies. The first step involved rapid chlorination of the surface Ga and As atoms to form surface bound mono- or dihalides :

$$Cl_2(g) + Ga\text{-}As(s) \longrightarrow GaCl_x(surf) + AsCl_x(surf) \qquad (1)$$

The second step, rate controlling at high pressure, produced readily vaporised $AsCl_3$ and surface bound $GaCl_3$:

$$GaCl_x(surf) + AsCl_x(surf) \longrightarrow AsCl_3(g) + GaCl_3(ads) \qquad (2)$$

The rate limitation encountered at high pressures was shown not to be caused by the build-up of a $GaCl_3$ layer. Since higher etch rates could be attained when atomic Cl was the etchant, they considered that the reaction was not limited by any process occurring after the products were formed. The low pressure rate-limiting reaction was thought to be the formation at reaction sites of products, such as Ga_2Cl_6. The etch rate was believed to reach the maximum once these sites were saturated, that is at high pressures.

A study by Furuhata et al[40] considered Cl_2 chemical dry etching of GaAs under high vacuum conditions (Cl_2 pressure between 8×10^{-5} and 1×10^{-3} Torr.) They found three distinct reaction regimes for the {100} plane. Below 150°C, etch rates showed a 0.6 order dependency on the pressure of chlorine and the activation energy for the process was calculated to be 42 kJ mol^{-1}. Between 150 and 450°C, there appeared to be little temperature dependence. Above 450°C, an activation energy of 67 kJ mol^{-1} was measured. They attributed these observations to the rate being limited by the desorption of various $GaCl_x$ products (as $AsCl_x$ products are known to be more volatile). Below 150°C they suggest the etch rate is limited by $GaCl_3$ desorption and that above 450°C the rate is limited by GaCl desorption. The relative etch rates of GaAs planes was found to differ slightly from that proposed by Ibbotson et al in that the rates for {100} and {110} were found to be equivalent.

Balooch and Olander[41] studied the reaction of {100} GaAs with molecular chlorine, with and without simultaneous bombardment by energetic argon ions. They proposed that at 27°C, ion bombardment accelerated the etch rate by a factor of six and attributed this mainly to the rapid removal of a scale of relatively non volatile $GaCl_3$ from the reacting surface. Without ion bombardment, the low thermal desorption

rate constant of $GaCl_3$ molecules in the surface scale was thought to cause accumulation on the GaAs substrate and the limiting of the reaction rate. The dimerisation step proposed by Ibbotson and Ha was not mentioned.

Ibbotson et al observed that at a temperature of 25°C, samples being etched in a bromine plasma were totally coated by a liquid layer, believed to be a gallium bromide reaction product and etching was negligible. Ha reported the formation of a liquid layer at temperatures between 25 and 70°C and high pressures of chlorine (over 15 Torr), which resulted in an unusual etch profile : etch depth was greatest at the sides of the profile.

Morphology of the etch was found to depend on the temperature: Ibbotson et al reported a rough to smooth transition at 125°C in a chlorine plasma whereas Ha found that shiny surfaces were produced at 160°C and above for molecular chlorine etching.

1.8 PURPOSE OF STUDY

The objective of the study described in this thesis was a determination of the pressure and temperature dependencies of the etching of GaAs {100} by molecular and atomic bromine.

Since molecular etching effects are often neglected in ion and plasma etching studies, a secondary objective was to determine whether there is a significant contribution by molecular bromine to such etching processes.

2 EXPERIMENTAL

2.1 MATERIALS

The bromine used in these studies was A.C.S. reagent grade (Aldrich) with a quoted purity of 99.5%. To fill a reservoir, it was first evacuated, the inlet was immersed in bromine and the tap was opened. In order to prevent contamination by water, calcium oxide was used as an in situ drying agent. The bromine was then frozen using an acetone and solid carbon dioxide bath and the air was pumped off. After thawing with a heating gun, this freeze-pump-thaw cycle was repeated twice more.

The gallium arsenide samples were cut from 5 cm diameter {100} wafers. GaAs {100} was the subject of the study since this plane is the most widely used in industry. Both undoped and silicon doped wafers were used and were supplied by Bell Northern Research. The Si doped samples had a doping concentration of 2×10^{16} atom cm^{-3}. Sample chips were generally rectangular and had a surface area of 0.1 to 0.2 cm^2. Some GaAs samples were masked with silicon nitride (Si_3N_4) stripes, by the U.B.C. Centre for Advanced Technology in Microelectronics. The stripes were 20 to 50 micrometres wide, spaced 100 micrometres apart and aligned with the $[\bar{1}10]$ or $[\bar{1}\bar{1}0]$ directions, if the surface is considered as the (100) plane. Wafer thicknesses were 0.25 and 0.5 mm.

2.2 MOLECULAR BROMINE ETCHING

2.2.1 Apparatus for molecular etching

The reaction system used (shown in schematic form in fig. 2.1) was constructed mainly of Pyrex glass. The reactor was made of 1.5 cm inner diameter, 1.8 cm outer diameter tubing and was 18 cm long. Most connecting tubing was 1.0 cm I.D. and 1.3 cm O.D.. Connections between sections of glassware were mostly made using Ace glass O-ring joints of 1.5 cm I.D.. Cajon Ultratorr O-ring joints were used for some glass-glass connections and all metal-glass connections. The bromine reservoir was connected to the system via a Matheson 602, 15 cm tube flowmeter, with glass float. The flowmeter was calibrated so that each reading on the meter corresponded to a flow in standard cubic centimetres per minute (sccm). The calibration was carried out by first calculating the volume (V) of the system from the dimensions of the components. This was found to equal 150 cm^3. Next, bromine was admitted at a certain flow reading and the pressure increase in the system was measured by connecting the pressure gauge (Edwards High Vacuum, 0-1000 Torr range) to a chart recorder (Hewlett Packard 680M strip chart recorder). The time for the pressure increase (dP/dt) was then related to the flow of gas (dn/dt), using the ideal gas law:

$$\frac{dn}{dt} = \frac{dP}{dt}\frac{V}{RT}$$

Flow rates were in the range of 10 to 70 sccm. Flow was adjusted so that the supply of gas exceeded that consumed in the etching reaction, by a factor of thirty or more.

A Sargent-Welch two-stage Duo-seal rotary vacuum pump (model 1400) with a pumping speed of 25 litres min^{-1} was used in conjunction with a liquid nitrogen cold trap, which functioned as a cryogenic pump.

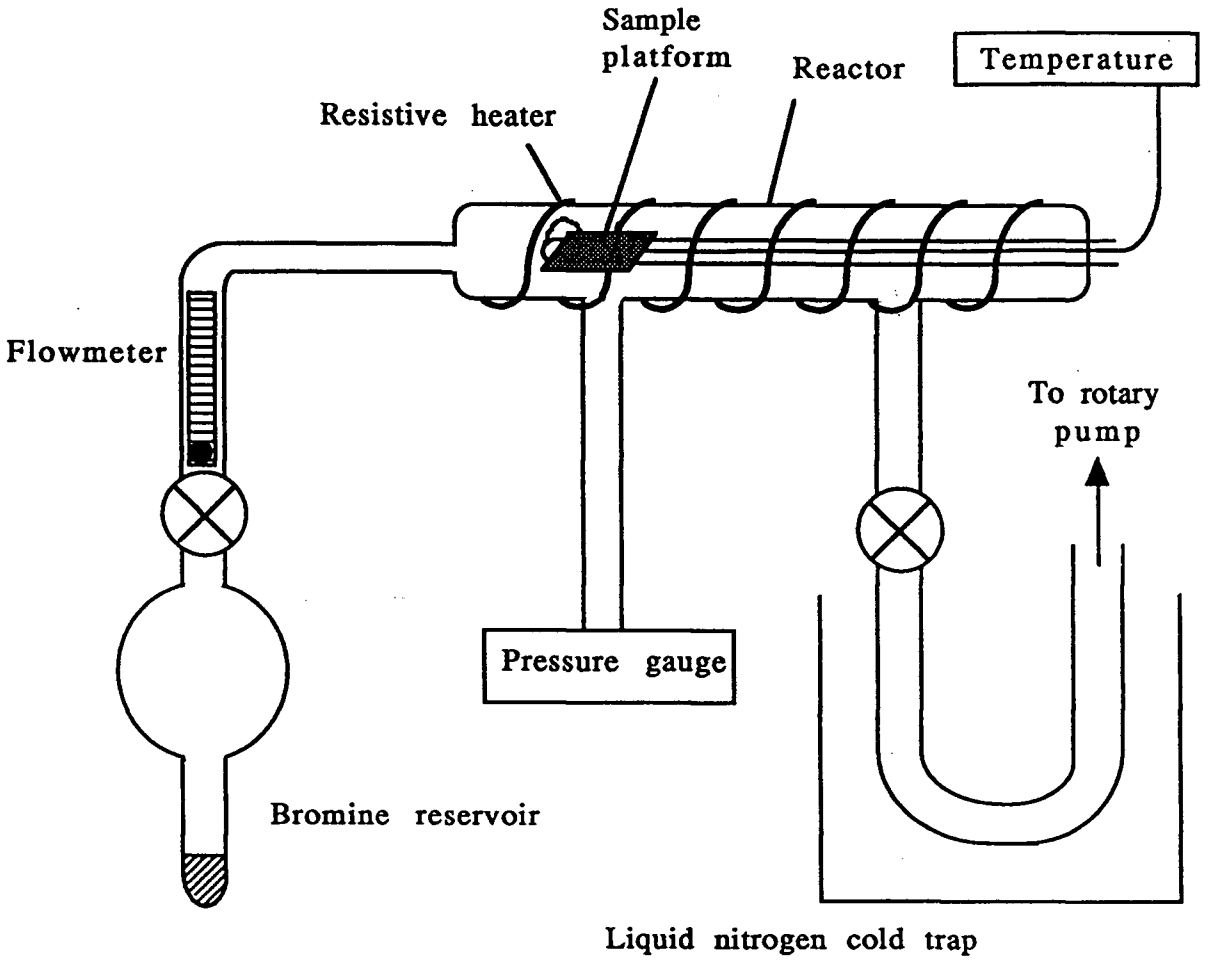

Figure 2.1 Schematic diagram of molecular bromine etching apparatus

The vacuum pump was connected to the glassware with 3cm O.D. heavy wall rubber tubing.

The samples were held by a glass spring onto a piece of thermally oxidised silicon, which acted as a heat sink (fig. 2.2). The silicon was mounted on a flattened portion of a thin walled glass tube, inside which was placed a chromel/alumel thermocouple. An alternative sample holder design proved unsuccessful. This involved the thermocouple being attached directly to the silicon platform with Torr Seal adhesive, which is a low vapour pressure resin suitable for vacuum systems. This arrangement would initially appear to give a more accurate temperature reading. However, the resin was quickly corroded by bromine. Furthermore, temperature readings from the new sample platform agreed closely with those measured in the alternative set-up.

2.2.2 Procedure for molecular etching

GaAs samples were immersed in concentrated hydrochloric acid for thirty seconds to remove any thick oxide layer and then washed with deionised water. Samples were then mounted on the platform, under a stream of nitrogen, and then the sample holder was placed in the reactor. The system was evacuated to approximately 10 milliTorr and a resistive heater was used to heat the reactor to the required temperature. Experiments were carried out at temperatures between 25 and 225°C. Next, bromine was flowed through the system at a steady flow and pressure and the time of exposure was recorded. This was usually 1 to 3 minutes. The flow and pressure of bromine could be adjusted with either the flowmeter valve or a valve before the cryogenic pump.

The etch rate was measured in one of two ways. For low etch rates a masked sample was used and the etch depth was measured by

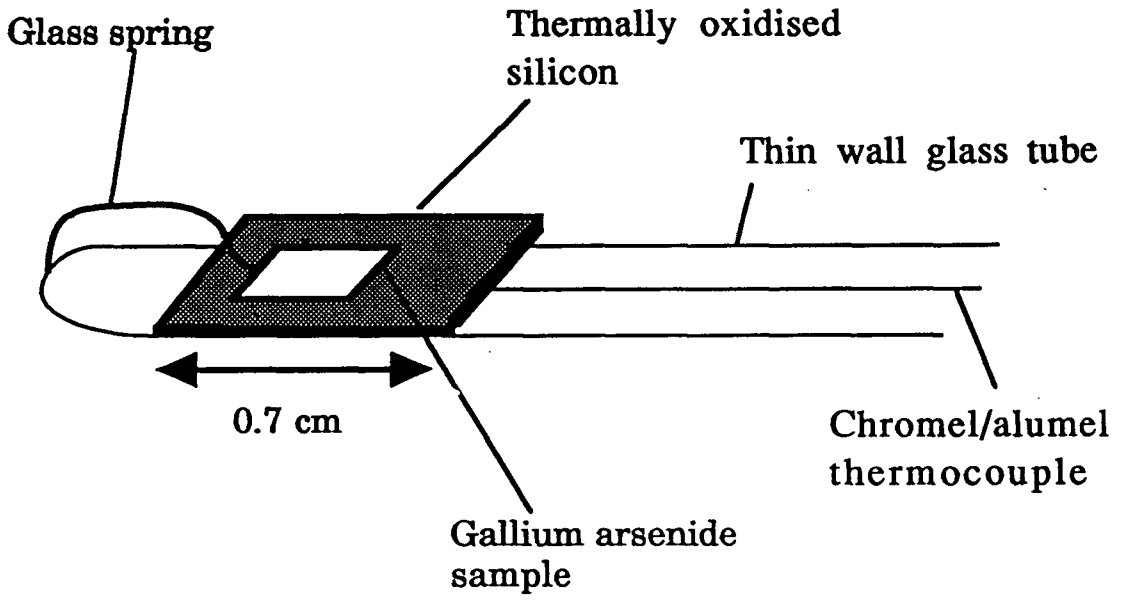

Figure 2.2 Sample platform

profilometry. The profilometer (Tencor alpha-step 200) scans along the surface with a very fine needle tip. The silicon nitride mask was aligned with the $[\bar{1}10]$ or $[\bar{1}\bar{1}0]$ direction, with respect to the (100) plane. Due to the different reactivity of the various planes of the GaAs structure, the mask can produce two etch profiles. As stated in section 1.2, when the mask is aligned with the $[\bar{1}\bar{1}0]$ direction, the faster etching As (111) planes are exposed on the etching of the (100) plane and a reverse mesa shape is produced: the profile has outward sloping walls. Whereas when the mask is aligned with the $[\bar{1}10]$ direction, the slower etching Ga (111) planes become exposed and cause the formation of V-shaped grooves. This crystallographic etching causes problems when trying to measure the etch rate of the (100) face. If reverse mesa formation occurs, the undercutting removes the mask once a limit of $(y\tan\theta)/2$ has been passed (fig. 2.3), where y = distance between stripes and θ = angle between (100) and (111) planes, 54.7°. Similarly, when V-shaped grooves form, the flat bottom of the profile (corresponding to the (100) plane) disappears when this limit is reached. Therefore a new method of etch rate determination was required to enable measurement of larger etch depths.

As etch rates were so high, relating the weight loss of the samples to the etch rate of the {100} plane was found to be an accurate method. The contribution to weight loss from the edges of the wafer was experimentally determined by sandwiching two wafers together and etching them at previously used conditions. The weight loss of the bottom wafer was due to etching from the edges only. For a sample of weight 0.0281 g, the weight loss from the edges was 0.0023 g. The expected weight loss from the {100} surface was 0.0047 g (calculated from the etch rate at these conditions determined by profilometry).

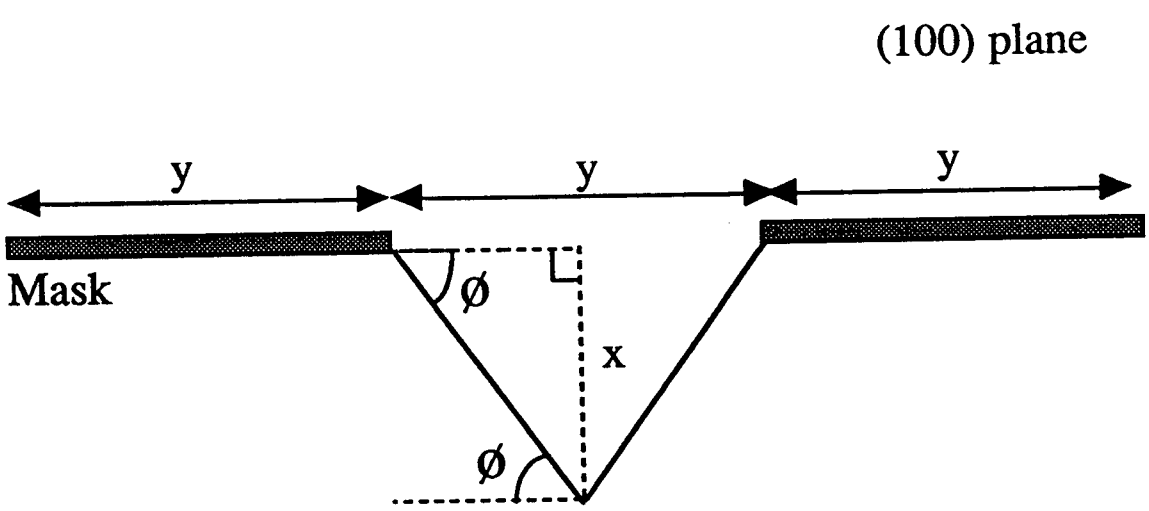

$$x = (y \tan \phi) / 2$$

$$x = 0.71\ y$$

Figure 2.3 Geometry of V-shaped groove formation

Therefore, the proportion of the apparent etch rate of the {100} plane due to the loss from the edges :

$$\%\,\text{of total weight loss, from edges} = \frac{0.0023}{0.0070} \times 100\%$$
$$= 33\%$$

This is within experimental error of the 40% expected from geometric calculations. These results showed that the weight loss from the edge planes could be compensated for by geometric calculations, as the etch rate of the edge plane was comparable to the etch rate of the top surface. The weight loss due to etching of the edges is proportionately less for larger samples and so correction factors were calculated for a range of sample sizes. These varied between 0.55 and 0.7 for the 0.5 mm thick wafer and was about 0.8 for the 0.25 mm thick samples.

Another method of etch rate determination that can be used for etch depths less than that specified above, is laser interferometry. This involves the detection of a laser beam reflected from a partially masked surface. As the wafer is etched the light reflected from the etched surface interferes with that reflected from the masked area. When the path difference is a multiple of half the wavelength of the laser light, the light waves interfere constructively and the photodetector response is at a maximum. However, in our studies it was found that the intensity of the reflected beam fell sharply as soon as the wafer was exposed to bromine and so the etch rate could not be monitored by this technique. This may have been due to (a) the shape of the etch trenches (b) the mask being too widely spaced or (c) the rapid formation of a poorly reflecting surface.

2.3 ATOMIC ETCHING

2.3.1 Apparatus for atomic etching

The reactor used in these experiments had a discharge region constructed of 1/2 inch O.D. quartz tubing, to withstand the high temperature of the discharge (fig. 2.4). Graded seals connected the discharge area to the Pyrex glass tubing. The distance from the discharge region to the sample platform was 13 cm. This was found to be short enough to prevent significant atom recombination but at the same time not cause overheating of the sample by heat generated by the discharge. A light trap was also incorporated between the sample platform and discharge so that light from the discharge was not detected in any attempt to monitor the glow due to bromine atom combination. A nitrogen gas inlet (Linde nitrogen) was positioned between the flow meter and the discharge region.

A Microtron 200 Watt, 2450 MHz microwave generator was used and the output was directed into the discharge region by an adjustable 1/4 wave coaxial cavity. Compressed air was blown through the cavity to cool the discharge area. The discharge was triggered using a handheld Tesla coil. The main advantages of a microwave discharge over a radio frequency discharge are that it is a very intense localised discharge with no tendency to spread and can be used at pressures of up to several Torr.[42]

The reactor was treated with phosphoric acid to 'poison' the walls and so reduce the degree of recombination of bromine atoms.[43] First the reactor was washed with a 5% solution of H_3PO_4 and then drained and left to stand for one hour. This produces a mildly acidic surface.

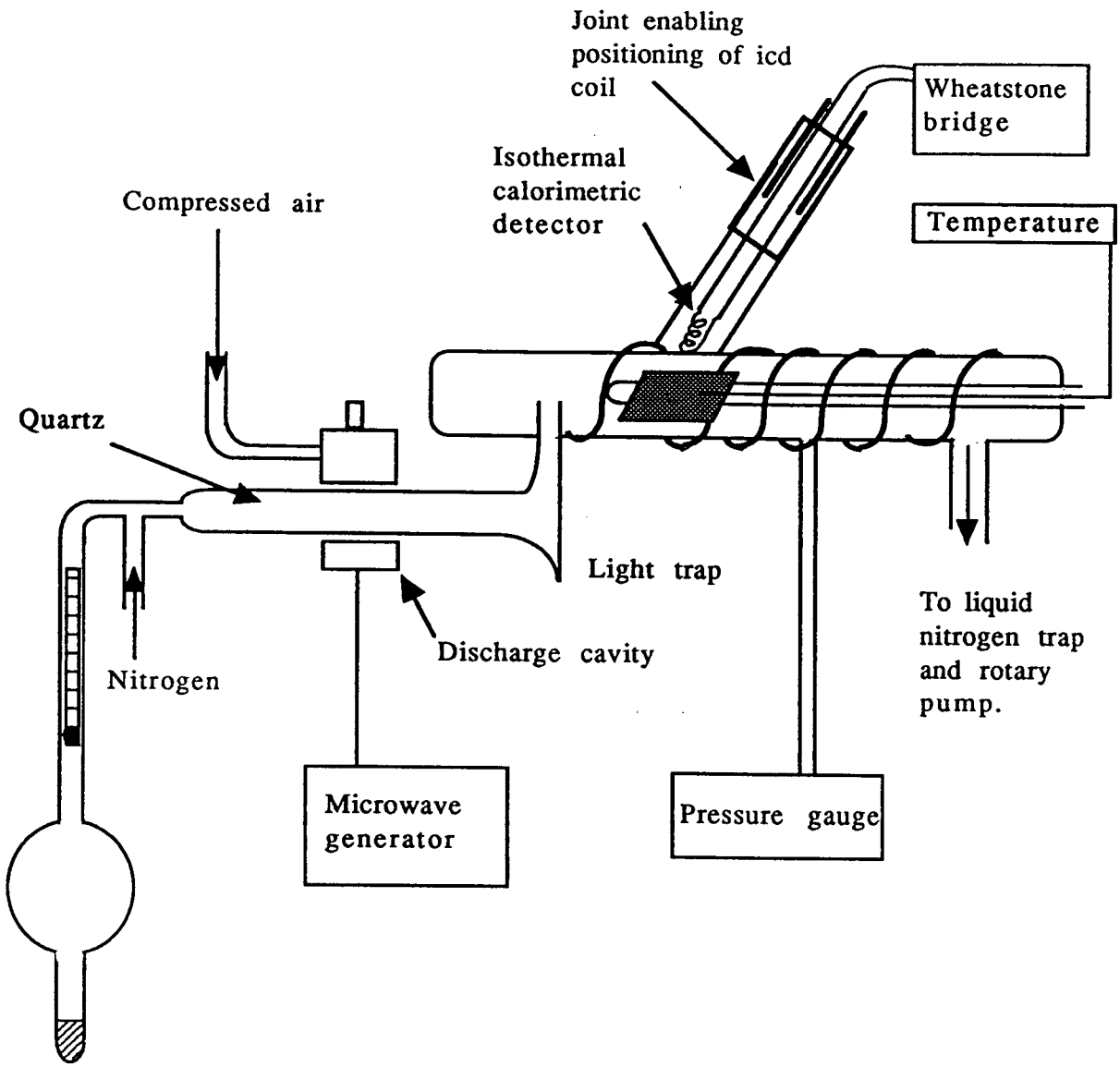

Figure 2.4 Schematic diagram of atomic etching apparatus

Then the discharge area was coated with concentrated H_3PO_4 and heated in a flame to produce a white coating of phosphorus pentoxide.

The absolute concentration of bromine atoms was measured with an isothermal calorimetric probe.[44] The probe usually consists of a platinum coil which is maintained at a given temperature by passing a current through it. The probe is placed in the gas flow as near as possible to the sample platform. When the discharge is in operation atoms recombine on the coil and so heat it. The electrical power supplied must be reduced to maintain it at the original temperature.

A platinum coil (99.99% purity, 0.25 mm diameter and 15 cm long) was spotwelded to two stainless steel rods (fig. 2.5). The coil was nickel-plated electrolytically as this has been found to produce the most efficient surface for bromine atom recombination. The rods were wrapped in teflon tape to prevent reaction of bromine with the metal and then set in a Pyrex tube, using Torr Seal for the vacuum seal. To minimise contamination by the resin it was only used at the end of the tube, 10 cm away from the coil. The probe was held in place by an O-ring arrangement and its position in the reactor was adjustable.

The resistance of the coil and the current passing through it were measured using a Wheatstone bridge set-up (fig. 2.6). First the bridge was balanced with bromine flowing over the coil. The current maintained the coil at a temperature of about 135°C. The voltage across the standard resistor was measured to determine the current passing through the coil (i_1) and the resistance of the probe (R) was found by measuring the resistance of the variable resistor. Then the discharge was started and the bridge was balanced again, by reducing the current. This reduced current value (i_2) is then used to calculate the atom flow :

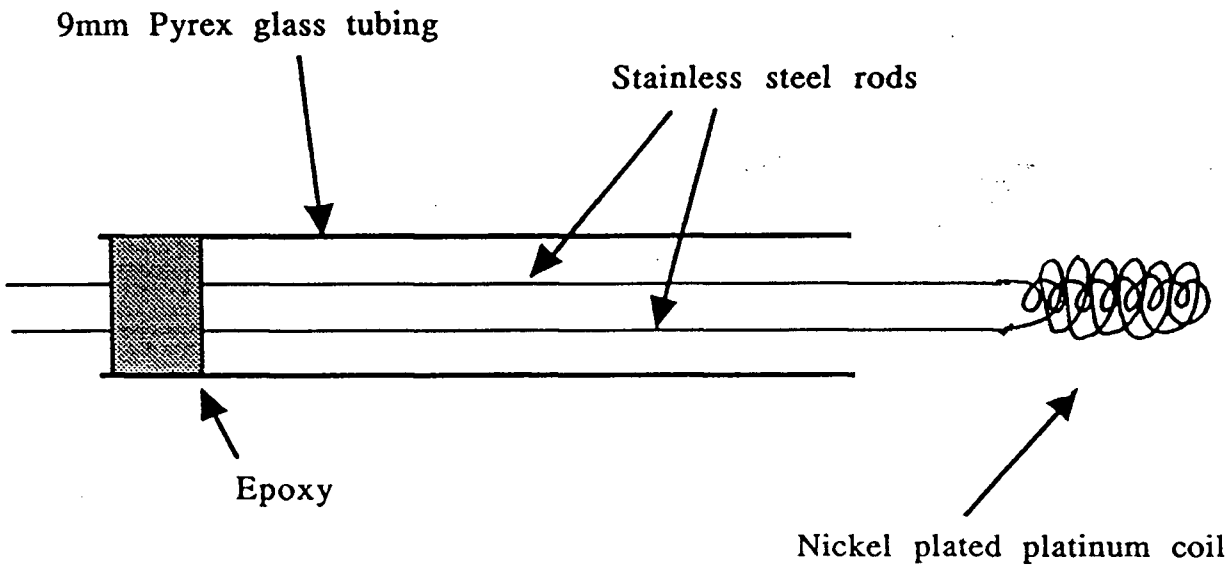

Figure 2.5 Isothermal calorimetric detector

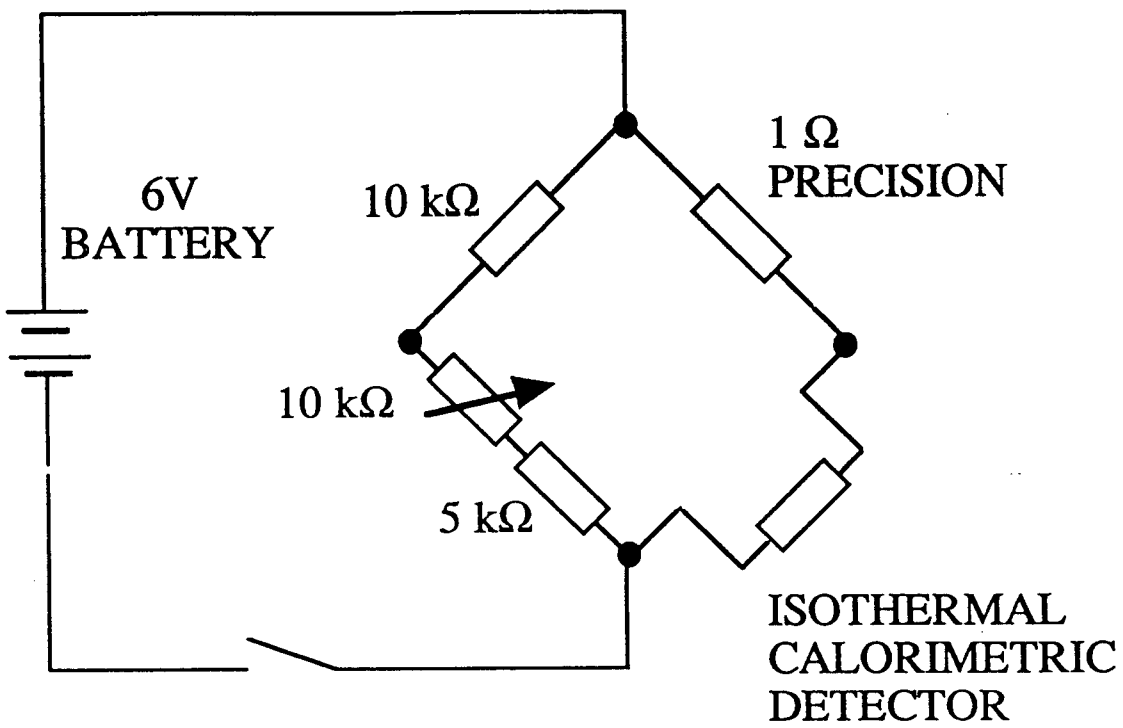

Figure 2.6 Wheatstone bridge arrangement for isothermal calorimetric detector

$$\text{Atom flow} = \frac{(i_1 - i_2)^2 R}{D/2} \text{ g atom s}^{-1}$$

where D = dissociation energy of bromine

= 193.9 kJ mol^{-1} [45]

The complete removal of atoms by the detector cannot be guaranteed unless two detectors are used in series. However, the coil was operated at the optimum temperature (determined by running the coil over a range of temperatures) and was coiled so as to occupy as much of the reactor's cross-section as possible. Furthermore, the concentration which we obtained compared well with concentrations measured by chemical titration of bromine atoms with NOCl in similar systems.[46]

2.3.2 Procedure for atomic etching

The measurement of atom flow could not be carried out during an etching experiment as balancing the Wheatstone bridge took several minutes. Therefore, the atom flow was measured before and after experiments and an average value was taken.

The glow emitted by the recombination of bromine atoms was considered as a way of monitoring the atom flow during each experiment. The response of a photodetector to the glow could be calibrated using the isothermal calorimetric probe. However, the cadmium sulphide detector proved too insensitive to measure the glow.

It was important to avoid contaminating the system with water since the phosphoric acid and phosphorus pentoxide would readily absorb water. This would be released again when the reactor is heated and the GaAs surface would be oxidised. This phenomenon was observed with the aid of a microscope set-up over the reactor. Interference fringes were seen as an oxide layer formed when the

discharge was started. The temperature was raised and when it reached a certain point (>100°C) the bromine atoms penetrated parts of the oxide layer and etching of the wafer could clearly be seen. Therefore, the reactor was only opened to the atmosphere after a positive pressure of nitrogen had been attained. The sample could then be loaded (after immersion in concentrated hydrochloric acid and rinsing with deionised water) as nitrogen flowed through the reactor. When the system had reached the required temperature, bromine was admitted at maximum flow, in order to maximise the number of atoms reaching the sample. The sample was exposed to molecules for up to half a minute before the discharge was started.

3 RESULTS

3.1 MOLECULAR BROMINE ETCH RATE DATA

Etch rates were measured at three temperatures : 125°C, 145°C and 183°C (tables 3.1, 3.2, 3.3). The data for the 125 °C series is plotted in fig. 3.1. At temperatures below 100°C, etching was very slow and above 200°C etch rates were too high and the possibility of insufficient reactant supply was encountered. In order to avoid the rate being limited by such factors, the ratio of bromine supplied to that required for the observed etch rate was kept as high as possible. This was done by maintaining maximum flow rates to keep this ratio thirty to one or greater.

Therefore, because of the above limitations the usable temperature range with this particular apparatus was normally 125°C to 183°C, although temperatures as high as 225°C could be used if the pressure was kept very low at the same time. Low temperature experiments were run as long as possible to give a reasonable etch depth.

The pressure of bromine in the system could be varied from 0.1 Torr to 20 Torr. The lower end of the range was determined by instrumentation limits : 0.1 Torr was the lowest pressure for which a consistent measurement could be maintained. Above 20 Torr, problems of insufficient bromine flow recur. High pressure combined with high temperature conditions resulted in the complete etching away of the thinnest GaAs samples, when measurable etch times were used.

Table 3.1 List of etch rates of GaAs (100) with Br_2 at 125°C

Etch rates from profilometry

Pressure (Torr)	Etch rate ($\mu m\ min^{-1}$)
0.1	0.8
0.2	1.7
0.3	1.9
0.4	2.8
0.4	2.9
0.5	4.2
0.5	3.4
0.6	5.6
0.7	5.4
0.8	7.1
0.8	7.1
0.9	5.1
1.0	8.8
1.1	9.1
1.2	11.1
1.4	13.0
2.0	17.9
2.6	20.5
2.8	17.1
3.3	21.4

Etch rates from weighing method

1.0	10.8
4.4	29.3
5.12	30.6
7.0	40.0
9.6	40.9
11.0	36.1
17.3	57.1
26.0	60.4

Table 3.2 List of etch rates of GaAs (100) with Br_2 at 145°C

Pressure (Torr)	Etch rate ($\mu m\ min^{-1}$)
0.2	2.6
0.5	7.2
0.8	13.8
1.0	15.1
2.3	16.5
2.3	21.6
2.3	20.0
5.3	36.7
7.0	41.0
11.0	51.0
15.0	51.5

Table 3.3 List of etch rates of GaAs (100) with Br_2 at 183°C

Pressure (Torr)	Etch rate ($\mu m\ min^{-1}$)
0.83	25.8
1.0	37.8
1.0	34.1
2.5	58.9
2.9	55.7
3.3	43.9
5.7	49.8
7.0	53.5
10.0	62.3
10.4	71.5
12.2	76.0
14.4	72.2
16.4	62.4
18.0	89.9
18.2	81.4
19.0	77.4
19.6	89.0

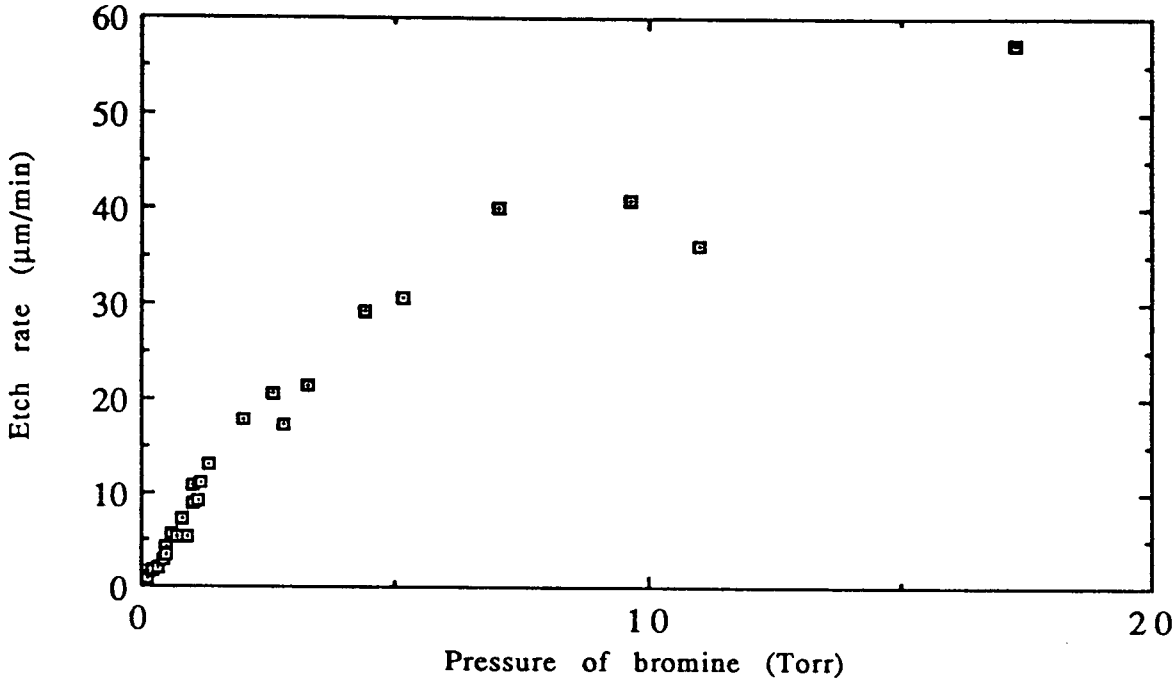

Figure 3.1 Graph of etch rate against pressure of Br_2 at 125°C

Profilometry was used for etch depth determination at pressures below 4 Torr, for the 125°C series and a typical etch profile is shown in fig. 3.2a. For higher etch rates, that is those at elevated temperatures and pressures, the use of masked samples was no longer feasible because of the limitation imposed by the crystallographic nature of the etch. This creates a V-shaped profile (fig. 3.2b) or a reverse mesa, both of which cause complete removal of the mask once a certain etch depth has been passed.

All other etch rates were measured by weight loss. Compensation for weight loss from the edges of samples was made by calculating surface areas and then applying a correction factor to the apparent etch rate. The etch rates determined by this technique compared well with those measured with a profilometer.

The morphology of the etch was not observed to change from rough to smooth at any specific temperature. However, high etch rates generally gave smoother etches.

3.2 ERROR ANALYSIS

The etch rates determined were weighted when plotted, with the reciprocal of ten percent of the etch rate. In this way the high etch rate data, which shows greater scatter, takes on a lower weighting. The figure of ten percent was arrived at by repeating several etching experiments under the same conditions. These showed 5 to 10 % difference in the measured etch rate. This is due to errors of about ±2 % in the pressure measurements, ±2% in temperature measurement and ±5% in the weighing technique.

A linear least squares analysis was performed on all etch rate-pressure data with errors accounted for in both the x and y values.[47]

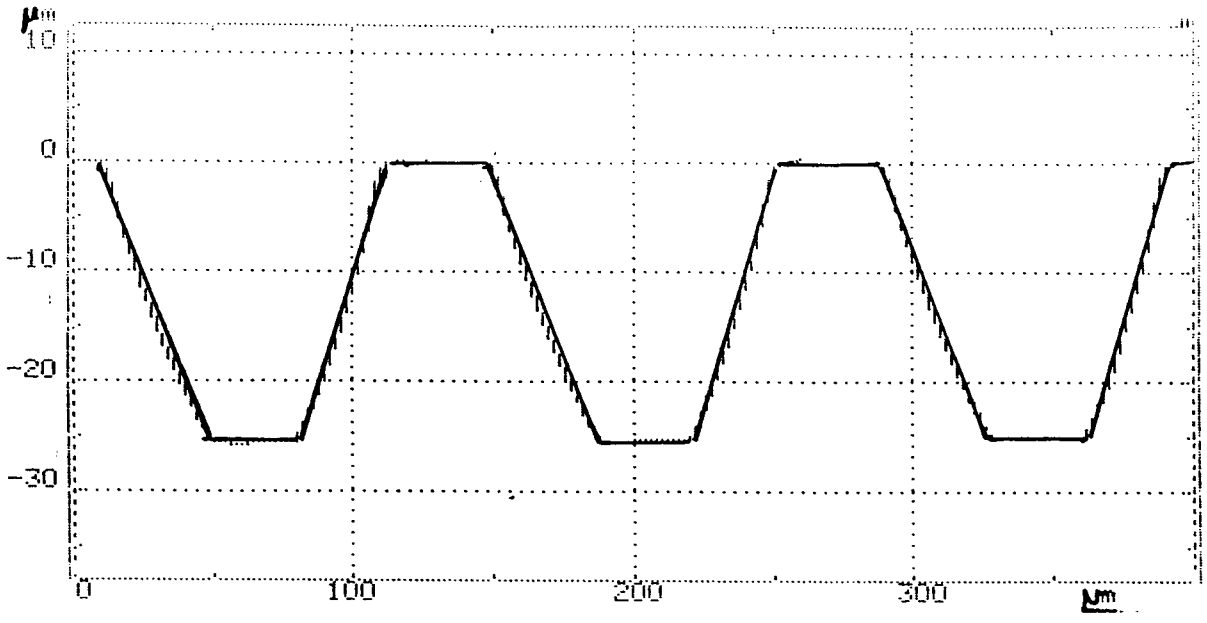

a) Run 62

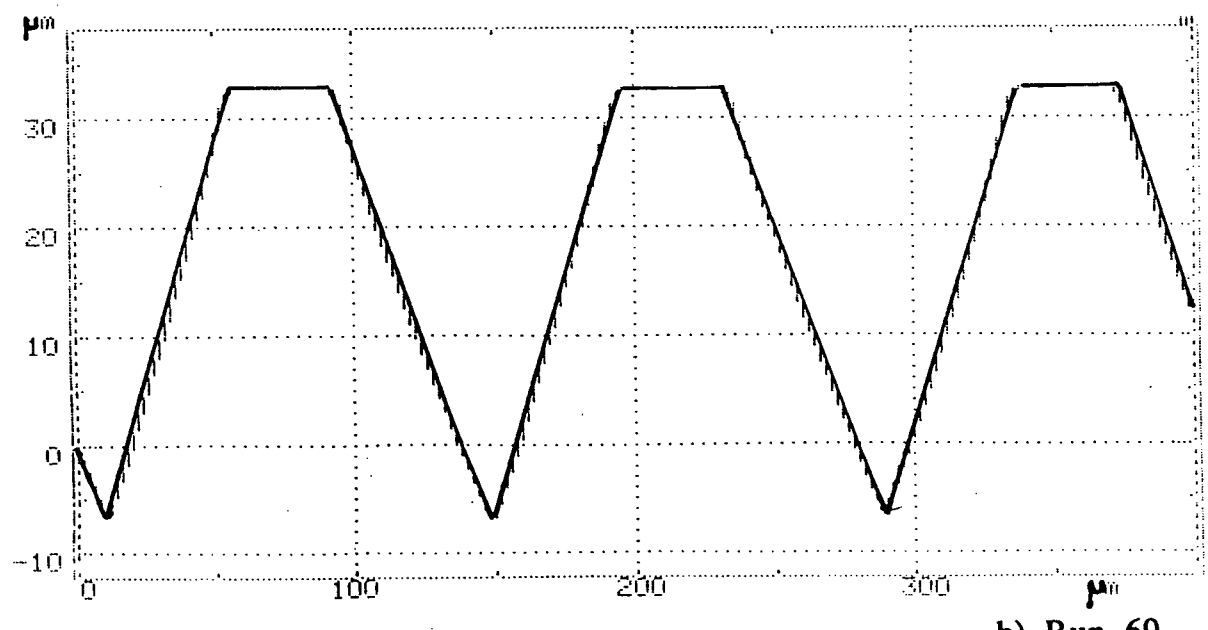

b) Run 69

Figure 3.2 Typical etch profiles obtained from profilometry

The errors in the gradients obtained in these graphs were then used as error bars in the subsequent Arrhenius plots. This provides an estimation of the errors (with 95% confidence) in the activation energies and pre-exponentials derived from the graphs.

In order to account for the possibility of irreproducibility being caused by defects in the wafer samples, two samples were etched simultaneously. The difference in measured etch rates was 8%, giving an overall error of ±4%, which is within the experimental uncertainty of the weight loss technique. Also the etch rates of the silicon doped GaAs samples, which have a dislocation density an order of magnitude higher than undoped sample, were no different than the undoped GaAs etch rates. This seems to confirm that surface defects do not play a significant role in determining bulk etch rates.

3.3 KINETIC ANALYSIS

The order of a reaction with respect to a particular gas phase reactant is the power to which the partial pressure of that reactant is raised in the rate law. Order can be determined by plotting natural logarithm of the rate against natural log of the pressure of that reactant. For example, if the rate law is given by :

$$\text{Rate} = k \left(P_{Br_2}\right)^n$$

then,

$$\ln(\text{rate}) = \ln k + n \ln P_{Br_2}$$

Therefore, the gradient of the line obtained by plotting ln (etch rate) against ln (pressure of Br_2) is equal to the order of the reaction with respect to Br_2. Such plots are shown in figs 3.3, 3.4 and 3.5 for 125°C, 145°C and 183 °C, respectively.

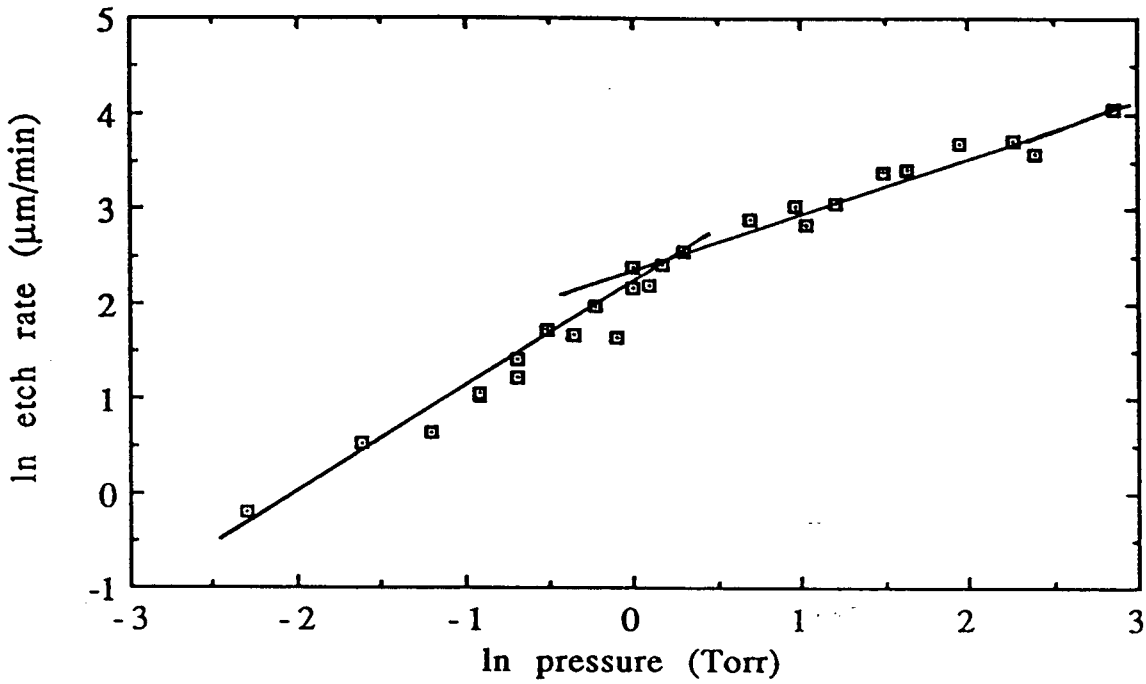

Gradients of lines are 1 and 0.5, approximately

Figure 3.3 Graph of ln etch rate against ln pressure of Br_2 at 125°C

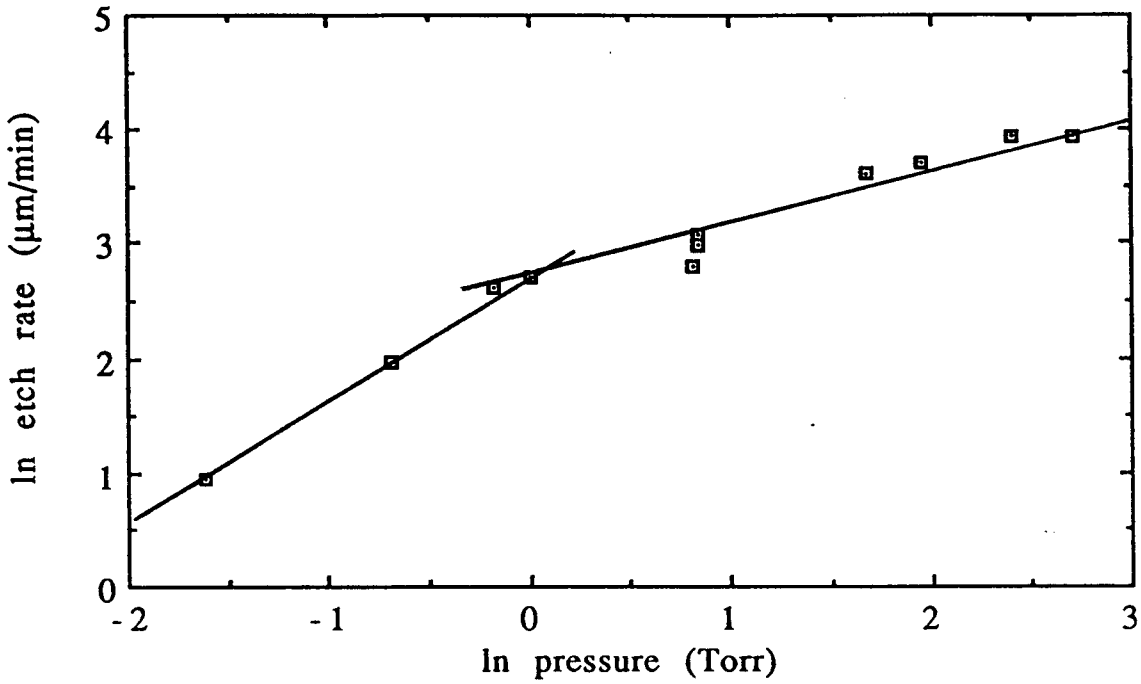

Gradients of lines are 1 and 0.5, approximately

Figure 3.4 Graph of ln etch rate against ln pressure of Br_2 at 145°C

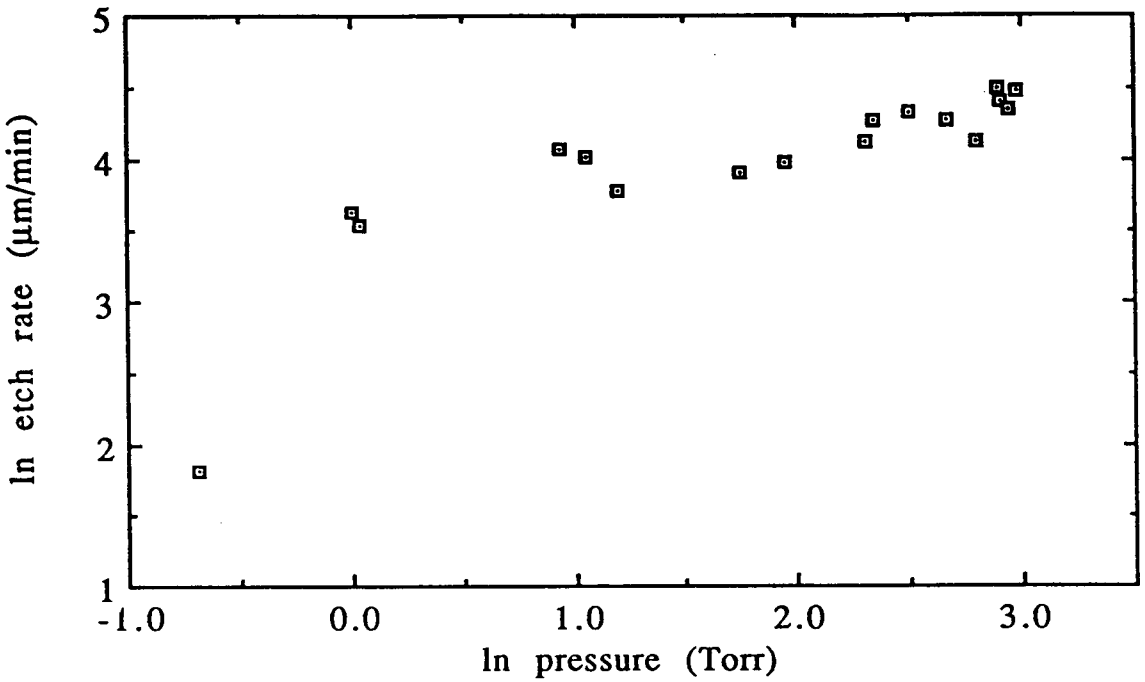

Figure 3.5 Graph of ln etch rate against ln pressure of Br_2 at 183°C

These graphs show two distinct regions. At a pressure of 1 to 2 Torr there appears to be a transition between two pressure dependencies. If these two regions are plotted separatedly (figs 3.6, 3.7), it can be seen that the low pressure region has an order of 1 and the high pressure region has an order of 0.5. Gradients for the three temperature series are presented in tables 3.4 and 3.5. The anomalously high value for the low presssure, 183°C readings can be attributed to the gradient being based on only three points.

A graph of etch rate against the square root of pressure should give a straight line for a half order reaction. Figure 3.8 shows such a graph for the high pressure region of the 125°C data. The data for the 125°C and 145°C series give small negative intercepts but that for the 183°C shows a small positive intercept.

Therefore we can represent the data by two empirical equations : At pressures below 1 to 2 Torr of bromine, where a is a first order rate constant :

$$\text{Etch rate} = a(P_{Br_2}) \qquad (3.1)$$

At pressures in excess of 1-2 Torr, where b is a half order rate constant and c is the negative intercept of the line drawn through the high pressure points on the half order graph :

$$\text{Etch rate} = b(P_{Br_2})^{1/2} - c \qquad (3.2)$$

3.3.1 Low pressure region

By plotting etch rate against pressure of bromine we can determine the rate constant in $\mu m\ min^{-1}\ Torr^{-1}$, at each temperature

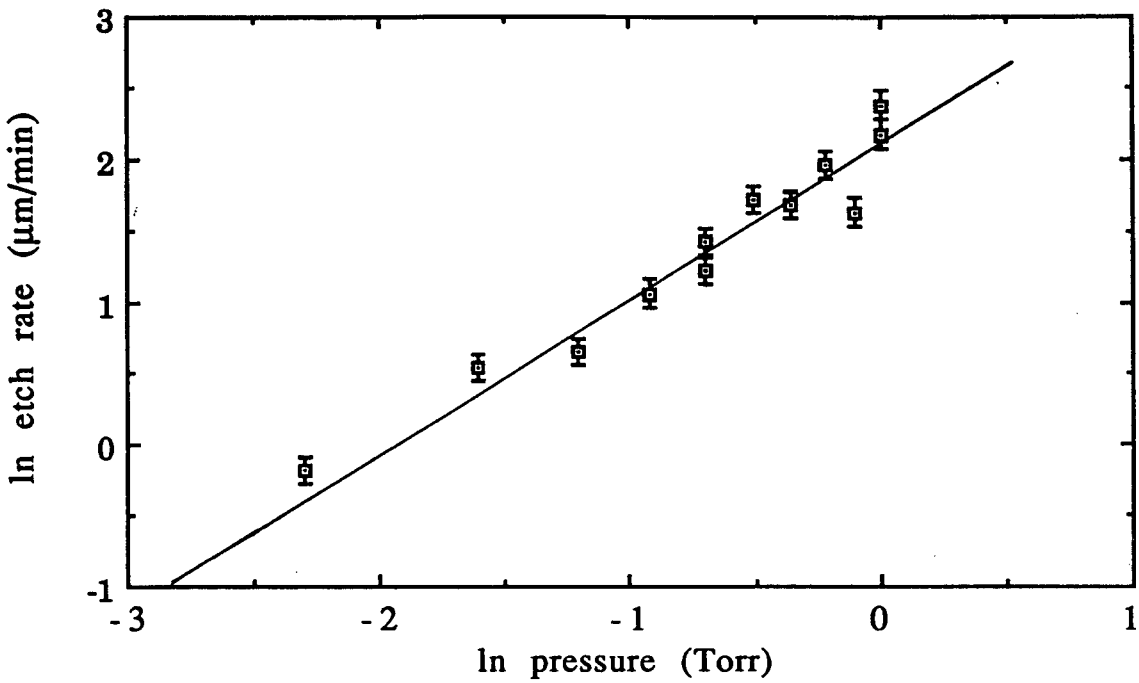

Gradient = 1.04

Figure 3.6 Graph of ln etch rate against ln pressure of Br_2 for the low pressure region at 125°C

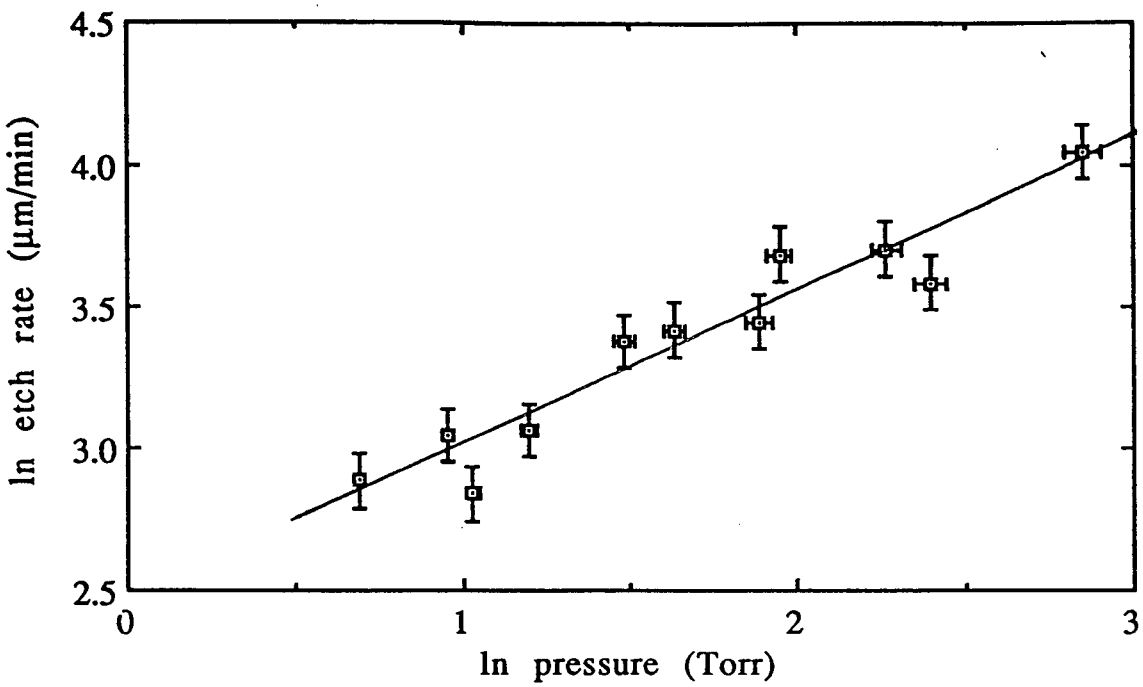

Gradient = 0.46

Figure 3.7 Graph of ln etch rate against ln pressure of Br_2 for the high pressure region at 125°C

Table 3.4 Gradients of ln etch rate versus ln pressure of Br_2 for the low pressure region

Temperature (°C)	Gradient
125	1.04
145	1.12
183	1.49

Table 3.5 Gradients of ln etch rate versus ln pressure of Br_2 for the high pressure region

Temperature (°C)	Gradient
125	0.46
145	0.58
183	0.47

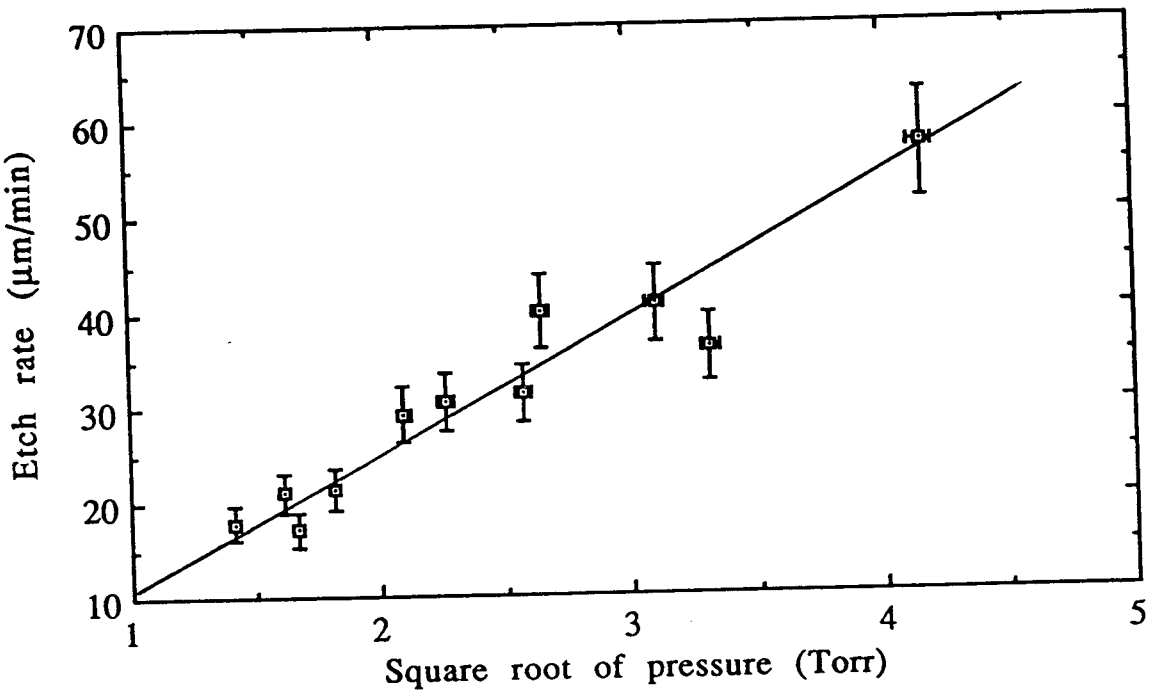

Gradient = 13.53
Intercept = -2.3

Figure 3.8 Graph of etch rate against square root of pressure of Br_2 for the high pressure region at 125°C

(Fig. 3.9, Table 3.6). If a single reaction step is rate limiting, the etch rate will exhibit an Arrhenius temperature dependency corresponding to this slow step. From the Arrhenius equation :

$$k = Ae^{-E/RT}$$

$$\ln k = \ln A - E/RT$$

where A = pre-exponential factor, E = activation energy and T = absolute temperature. The rate constants for etching experiments are most conveniently expressed in terms of the units used for measuring etch depth and pressure. A and E can be determined by plotting ln k against 1/T. Figure 3.10 shows the resultant graph and the values obtained from this are 33.8 ± 1.0 kJ mol^{-1} for the activation energy and (1.03 ± 0.3) x 10^{22} molecules cm^{-2} s^{-1} $Torr^{-1}$ for the pre-exponential factor.

Similar graphs can be constructed using (etch rate/pressure of bromine), which is equivalent to rate constant a in equation 3.1. Two such graphs were plotted for data at 0.83 Torr and 1.0 Torr (Tables 3.8, 3.9 ; figs 3.11, 3.12). These graphs show close agreement and give an average activation energy of 27.0 kJ mol^{-1}. Data obtained from all these Arrhenius plots is seen in Table 3.7. The average activation energy calculated from these three sets of data is 29.2 ± 4.0 kJ mol-1 and the average pre-exponential is (3.4 ± 4.4) x 10^{21} molecule s^{-1} cm^{-2} $Torr^{-1}$.

As these experiments were carried out at constant pressure, we actually derive an activation enthalpy from our data. However, the difference is only RT for a first order reaction and 1/2 RT for a half order reaction and this is within the experimental error.

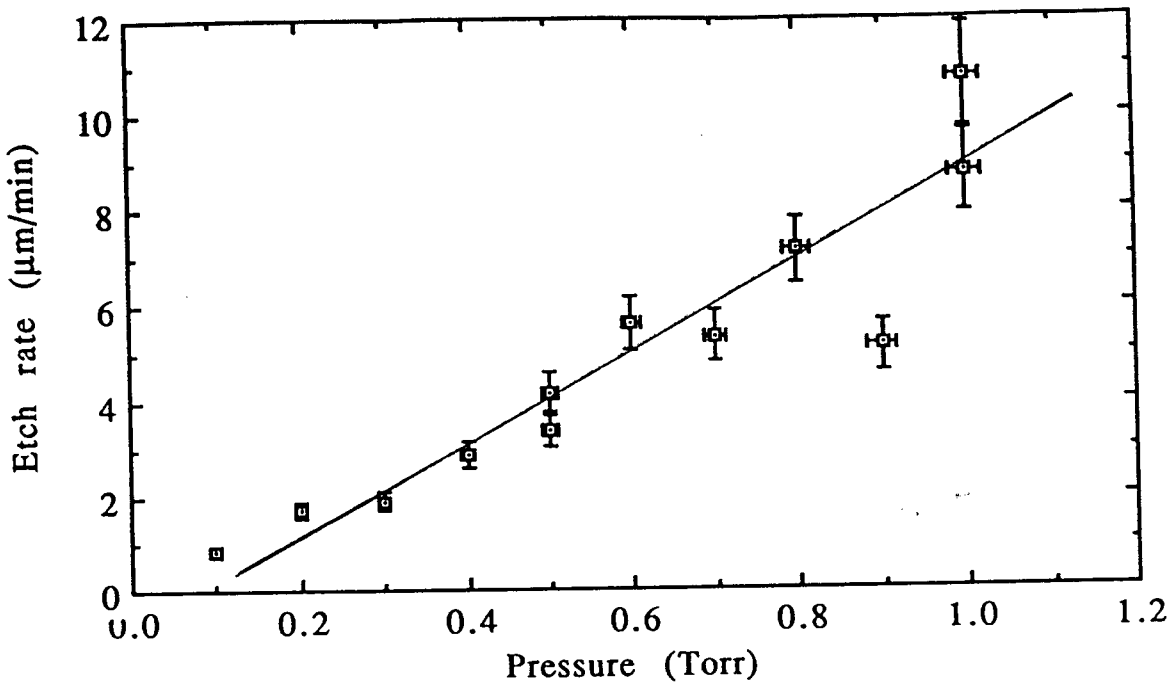

Gradient = 9.26 ± 1.1 μm min^{-1} $Torr^{-1}$

Figure 3.9 Graph of etch rate against pressure of Br_2 for the low pressure region at 125°C

Table 3.6 Gradients of etch rate plotted against pressure of Br_2 for the low pressure region

Temperature (°C)	Gradient ($\mu m\ min^{-1}\ Torr^{-1}$)
125	9.26
145	16.36
183	34.56

Table 3.7 Arrhenius data for the low pressure region

Pressure (Torr)	Activation energy ($kJ\ mol^{-1}$)	Pre-exponential factor (molecules $s^{-1}\ cm^{-2}\ Torr^{-1}$)
0.83	25.4 ± 2.6	$(9.31 \pm 9.7) \times 10^{20}$
1.0	28.6 ± 4.0	$(1.97 \pm 4.4) \times 10^{21}$
0 to 1 Torr => k values from gradients	33.8 ± 1.0	$(0.94 \pm 0.3) \times 10^{22}$

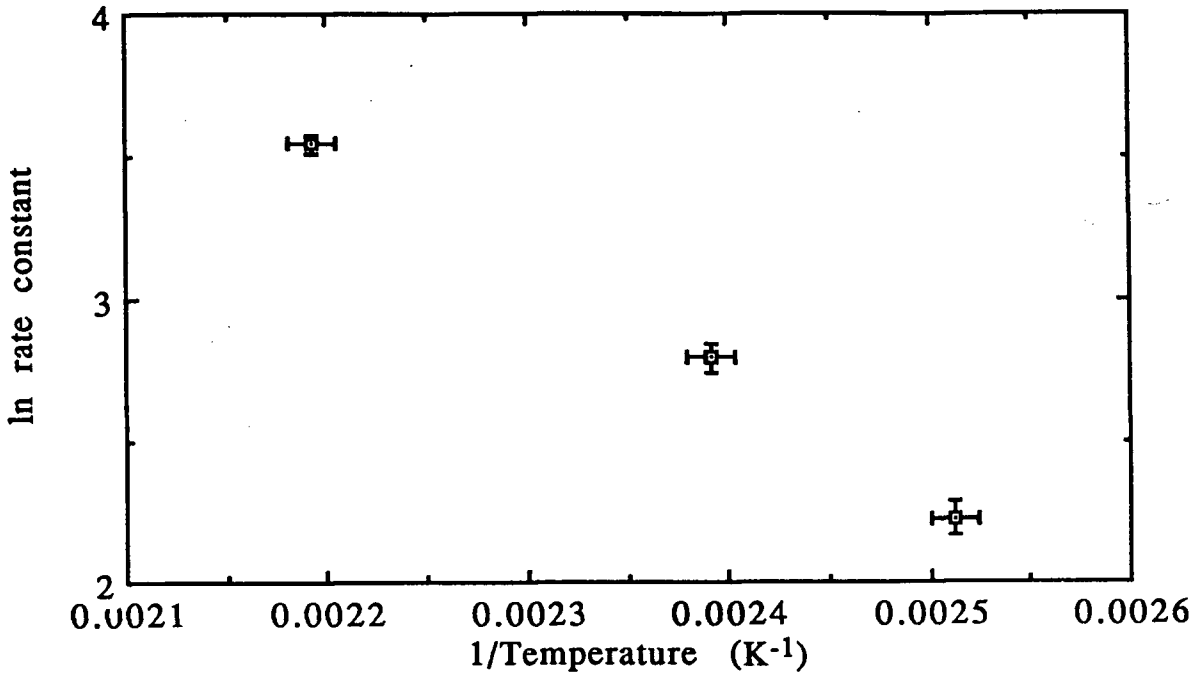

Gradient = -4060 ± 115 K
Intercept = 12.4 ± 0.3

Figure 3.10 Arrhenius plot for the low pressure rate constants

Table 3.8 List of etch rates for a Br_2 pressure of 0.83 Torr, at several temperatures

Temperature (°C)	Etch rate ($\mu m\ min^{-1}$)
117	9.4
129	10.0
151	12.3
171	23.6
202	37.3
231	47.1

Table 3.9 List of etch rates for a Br_2 pressure of 1.0 Torr, at several temperatures

Temperature (°C)	Etch rate ($\mu m\ min^{-1}$)
112	5.45
122	11.0
125	8.8
127	10.8
142	15.1
166	19.9
193	30.0

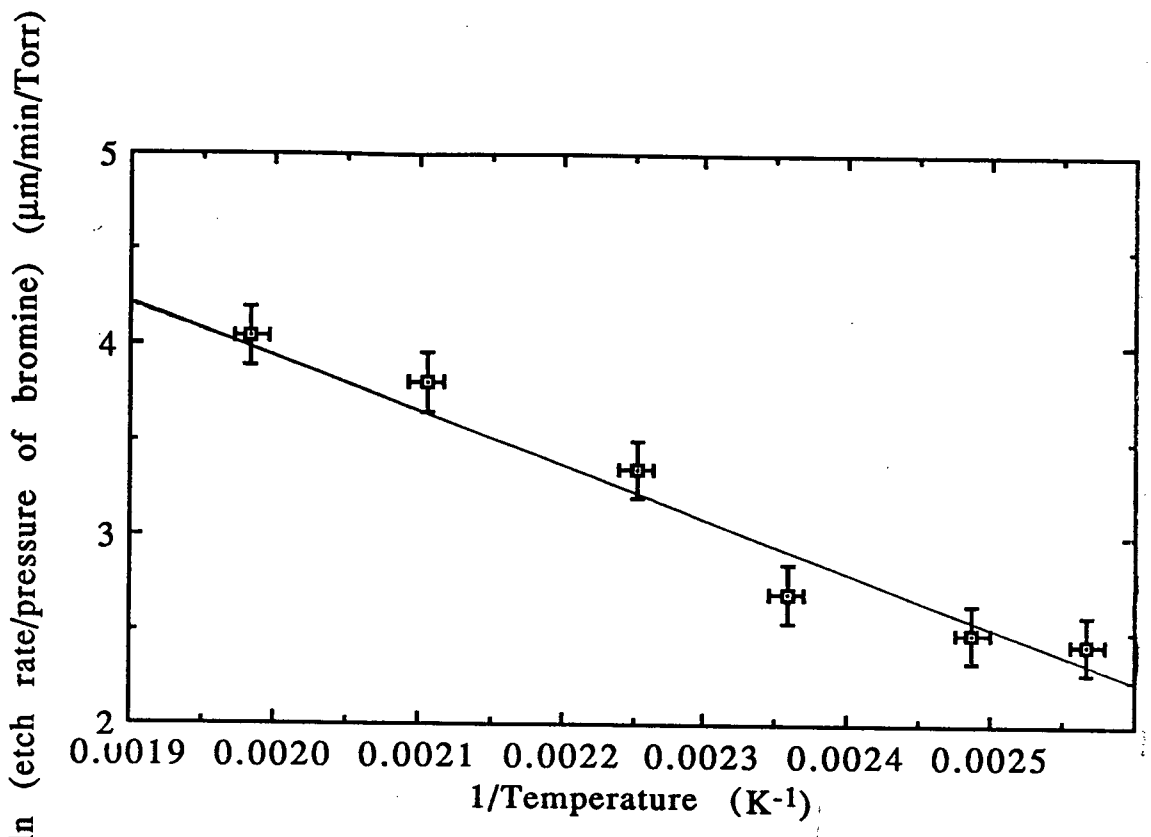

Gradient = -3052 ± 308 K
Intercept = 9.94 ± 0.7

Figure 3.11 Arrhenius plot for etch rates at a Br_2 pressure of 0.83 Torr

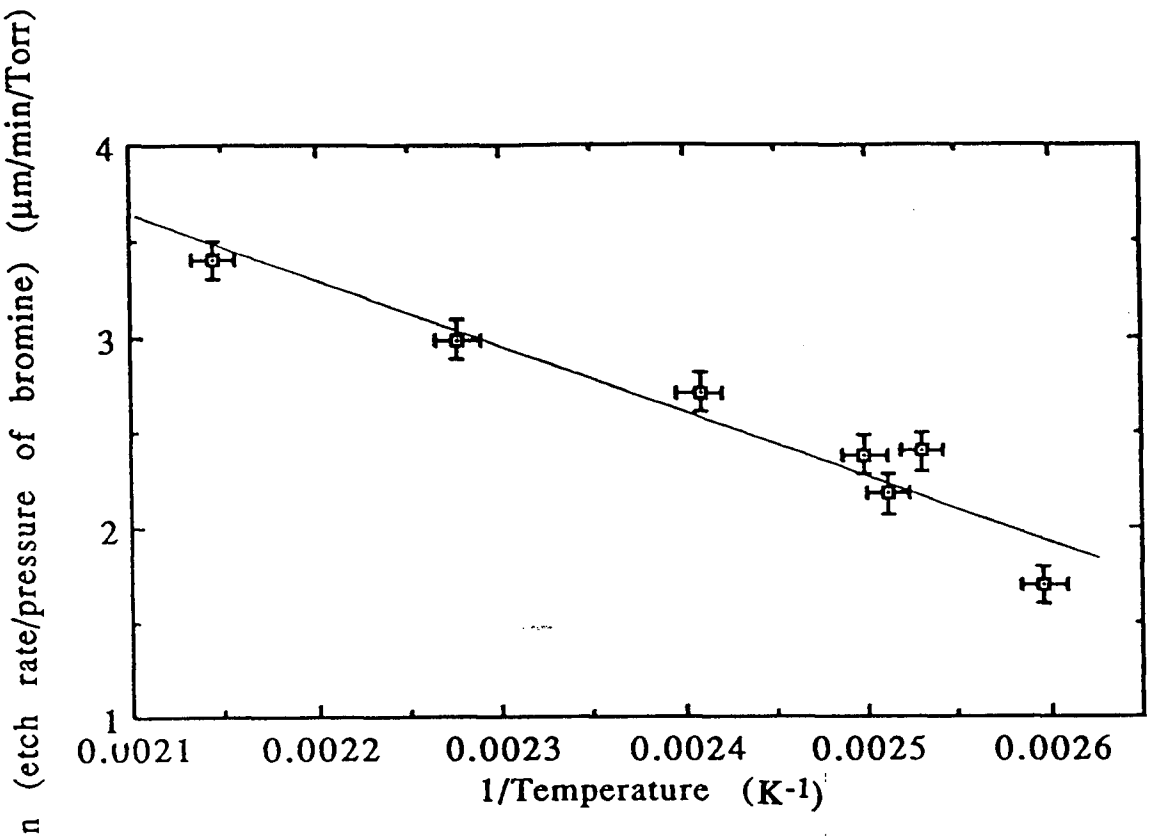

Gradient = -3443 ± 478 K
Intercept = 10.9 ± 1.2

Figure 3.12 Arrhenius plot for etch rates at a Br_2 pressure of 1.0 Torr

3.3.2 High pressure region

From the empirical equation 3.2, the constants b and c can be obtained by plotting etch rate against the square root of pressure (Table 3.10). The gradient b is a half order rate constant. Assuming an Arrhenius equation can be used to describe the temperature dependence then a plot of ln b against 1/T (fig. 3.13) gives an activation energy (8.4 ± 0.65 kJ mol^{-1}) and pre-exponential factor ((6.4.± 1.3) x 10^{18} molecules cm^{-2} s^{-1} $Torr^{-1/2}$) for the half order rate constant.

3.4 ATOMIC ETCHING

Atomic etching was carried out at 0.83 Torr of bromine (Table 3.11), a pressure at which a series of molecular etches had been carried out. Therefore compensation for the etching due to bromine molecules could readily be carried out. The concentration of atoms obtained varied between 12 and 15%. Assuming that the atomic etching reaction is first order, the rate constant can be calculated by first correcting for the etching by molecules and then dividing the atomic etch rate by the partial pressure of bromine atoms. Figure 3.14 shows an Arrhenius plot in which the ln of the rate constant is plotted against the reciprocal of temperature. This gives an activation energy of 12.9 ± 0.9 kJ mol^{-1} and a pre-exponential factor of (7.1 ± 2.0) x 10^{20} atom s^{-1} cm^{-2} $Torr^{-1}$.

3.5 ANALYTICAL RESULTS

After several etching experiments, a brown deposit appeared downstream of the sample platform, on the periphery of the heated region of the reactor. This was dissolved in acetone and analysed by electron ionisation mass spectrometry. The most prominent peaks were

Table 3.10 Gradients and intercepts of the graphs of etch rate versus (pressure of bromine)$^{1/2}$, for the high pressure region

Temperature (°C)	Gradient b	Intercept c
125	13.53	-2.3
145	15.03	-5.7
183	18.99	4.00

Table 3.11 List of etch rates for GaAs (100) with Br, at a Br_2 pressure of 0.83 Torr

Partial pressure of Br atoms (Torr)	Temperature (°C)	Etch rate (corrected) ($\mu m\ min^{-1}$)
0.12	89	30.2
0.15	102	43.0
0.10	178	75.7
0.16	204	95.8
0.12	206	98.9
0.12	229	104.2

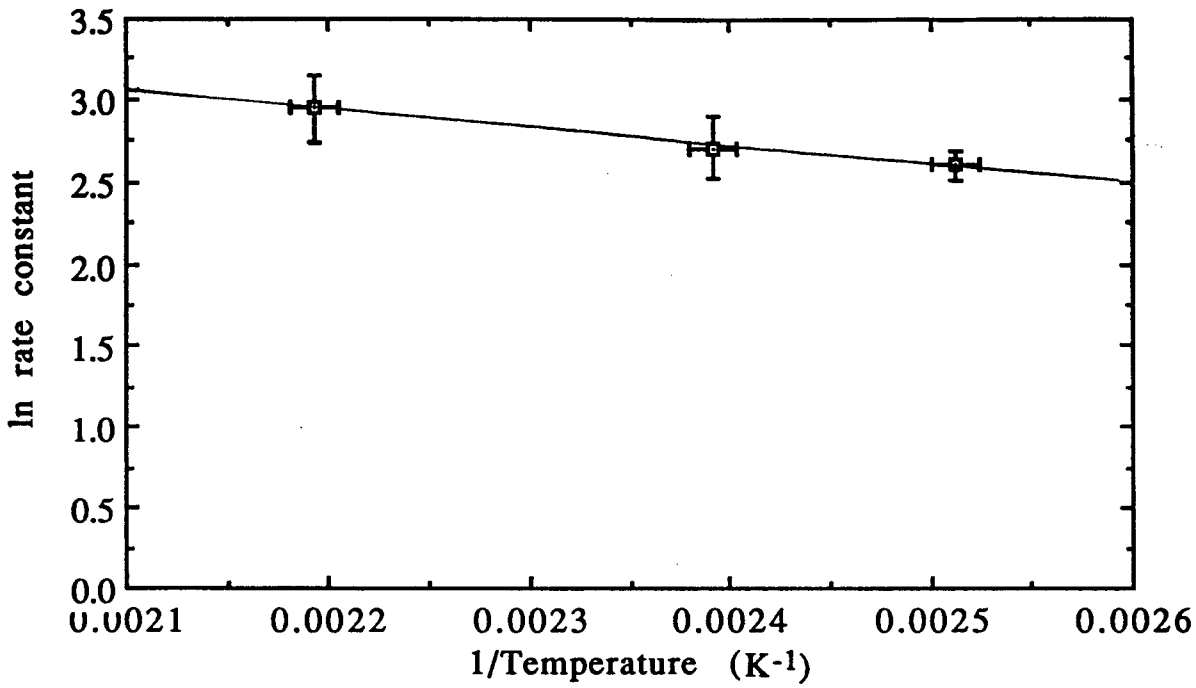

Gradient = -1014 ± 78 K
Intercept = 5.2 ± 0.2

Figure 3.13 Arrhenius plot for the high pressure rate constants

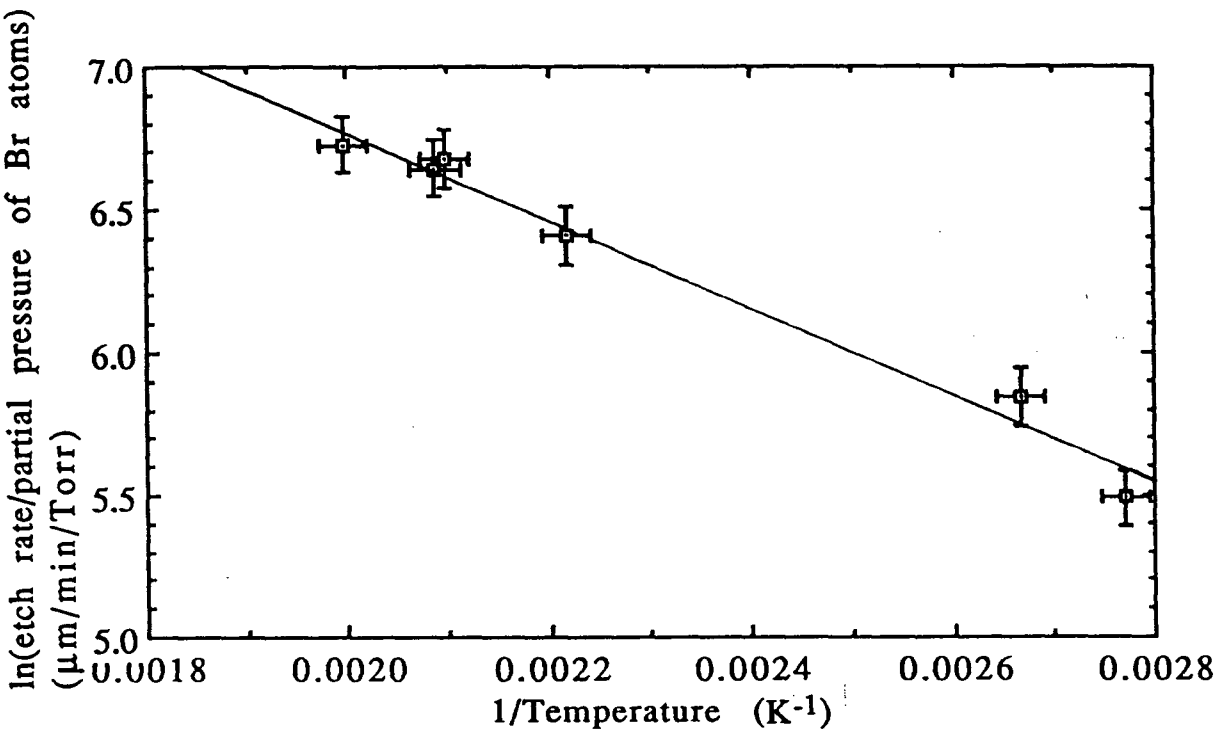

Gradient = -1548 ± 104 K

Intercept = 9.9 ± 0.2

Figure 3.14 Arrhenius plot for atomic etching rate constants

those due to gallium tribromide and its fragments. No peaks were found for the equivalent arsenic compounds.

An etched wafer was analysed by X-ray analysis (EDX) using a scanning electron microscope (Hitachi S-579). The atomic percentage of gallium was found to be 52.3% and that for arsenic 47.7%. This corresponds to 50.6 wt% gallium and 49.6 wt% arsenic. As the accuracy of the analysis is given as within 0.5 wt% it can reasonably be concluded that the sample surface remained equimolar. No traces of bromine were detected. This analysis probes to a depth of about 1 μm.

4 DISCUSSION

4.1 PROPOSED MECHANISM

The reaction of GaAs {100} with bromine displays two distinct pressure dependencies. At bromine pressures below 1-2 Torr, the reaction is first order with respect to the concentration of bromine. When the pressure exceeds 1-2 Torr, the reaction becomes half order. A mechanism involving several steps is needed to account for this behaviour.

The adsorption of molecular chlorine on the {110} surface of GaAs has been studied by a number of spectroscopic techniques.[48] The surface was found to be rapidly saturated with chlorine, which is initially non-dissociatively adsorbed. The chlorine subsequently dissociates and is chemisorbed on the GaAs surface. Assuming this occurs for bromine on {100} GaAs also, then a brominated surface is produced, in a rapid Langmuir type process. A physically adsorbed layer of bromine molecules may form initially but this should be a rapid process with no significant activation energy and hence not rate controlling. The surface will consist of $GaBr_x$ and $AsBr_x$ species, where x is 1 or 2. From steric considerations, the surface Ga and As atoms on a {100} surface are most likely to be monosubstituted.

In order to explain the rate laws observed in the present study we propose the following rate controlling steps :

$$Br_2(g) \underset{k_{-1}}{\overset{k_1}{\rightleftharpoons}} 2Br(ads) \qquad (4.1)$$

$$Br(ads) \xrightarrow{k_2} Products \qquad (4.2)$$

The first step is the reversible dissociative adsorption of bromine molecules on the already halogenated gallium arsenide surface. The second step (reaction 4.2) represents the reaction of one of these adsorbed atoms with the halogenated surface to produce gaseous product or at least some intermediate which yields gaseous products in a non rate-determining step. The mechanism can be considered a variation of the Eley-Rideal mechanism since it postulates that a mobile, weakly adsorbed layer of bromine atoms is involved in the product formation.

The products are likely to be $AsBr_3$ and Ga_2Br_6. $AsBr_3$ is the only stable arsenic bromide.[49] $AsBr_3$ is volatile and it should desorb rapidly. Therefore the desorption of the arsenic product should not limit the rate of reaction. Ga_2Br_6 is the most stable gallium bromide near room temperature but it is less volatile than $AsBr_3$. At the boiling point of the gallium bromide (279°C) it has been shown that 70% of the bromide exists as the dimer.[50] The vapour pressure of $GaBr_3$ is given by[51] :

$$\log P^* = (-14{,}300/4.57T) + 8.554$$

At the melting point of $GaBr_3$ (122-124°C), the vapour pressure is 5.4 Torr. From the kinetic theory of gases :

$$Re = \alpha\ (M/2\pi RT)^{1/2}\ P^*$$

where α = coefficient of condensation

M = molecular weight

and R,T have their usual meanings.

The coefficient of condensation typically falls between 0.1 and 1.0.[52] Taking α as 0.1 gives the minimum evaporation rate, which is

calculated as 0.028 g cm^{-2} s^{-1}. This is equivalent to an etch rate of 3100 μm min^{-1}, which is two orders of magnitude higher than the etch rates observed at this temperature. So the desorption of Ga_2Br_6 molecules from a $GaBr_3$ liquid layer can be dismissed as a possible rate determining step, in the same way as Ibbotson et al discounted Ga_2Cl_6 vaporisation as rate limiting, in their studies using a chlorine plasma.

The atomic etching experiments gave faster rates than molecular etching (though this could only be explored for the low pressure region) and so, assuming the products of the reaction are the same, this supports the argument that product desorption is not rate limiting

Diffusion limitations can arise at the pressures used in this study. However, it was found firstly that no levelling off of etch rate was seen at pressures up to 40 Torr at 125°C. Secondly, the flow rate was not found to influence the etch rate. In a diffusion limited reaction the rate is determined by how fast the reactant is delivered to the surface and this can be dependent on flow.

4.2 KINETIC ANALYSIS OF MECHANISM.

If equations 4.1 and 4.2 represent the rate controlling steps :

$$Br_2(g) \underset{k_{-1}}{\overset{k_1}{\rightleftharpoons}} 2Br(ads) \qquad (4.1)$$

$$Br(ads) \xrightarrow{k_2} \text{Products} \qquad (4.2)$$

Then the etch rate is given by the rate of formation of products :

$$\text{Etch rate} = \frac{d(\text{Product})}{dt} = k_2[Br(ads)] \qquad (4.3)$$

where [Br(ads)] = concentration of adsorbed bromine atoms.

During the steady-state etching reaction :

$$2k_1P - 2k_{-1}[Br(ads)]^2 - k_2[Br(ads)] = 0 \qquad (4.4)$$

where P = pressure of bromine.

Solving this quadratic equation for [Br(ads)] :

$$[Br(ads)] = \frac{-k_2}{4k_{-1}} + \frac{\left(k_2^2 + 16k_{-1}k_1P\right)^{1/2}}{4k_{-1}} \qquad (4.5)$$

Substituting from (4.5) into (4.3) gives :

$$\text{Etch rate} = \frac{k_2^2}{4k_{-1}}\left(1 + \frac{16k_{-1}k_1P}{k_2^2}\right)^{1/2} - \frac{k_2^2}{4k_{-1}} \qquad (4.6)$$

In the low pressure region :

As $(1 + x)^{1/2} \simeq (1 + x/2)$ when x is small, then at low pressures :

$$\left(1 + \frac{16k_{-1}k_1P}{k_2^2}\right)^{1/2} \simeq \left(1 + \frac{8k_{-1}k_1P}{k_2^2}\right) \qquad (4.7)$$

This approximation arises from the back reaction in the equilibrium between the bromine molecules and the weakly adsorbed Br atoms (4.1) being negligible relative to the rate of reaction 4.2 for the low pressure region. By substituting into 4.6 from 4.7, we find :

$$\text{Etch rate} = 2k_1P \qquad (4.8)$$

We can compare this etch rate equation with the empirical equation 3.1 :

$$\text{Etch rate} = a(P_{Br_2}) \qquad (3.1)$$

Then it can be seen that $a = 2k_1$. Therefore from the values obtained for this constant a (section 3.3.1) the rate controlling reaction step can be presented in the form of an Arrhenius equation, for the pressure range 0-2 Torr and temperatures from 100 to 200°C :

$$k_1 = 4.1 \times 10^5 \ \mu m \ min^{-1} \ Torr^{-1} \ e^{(-29.2 \ kJ/mol)/RT}$$

At high pressures:

$$\frac{16 k_1 k_{-1}}{k_2^2} >> 1 \qquad (4.9)$$

Substitution from 4.9 into 4.6 yields :

$$\text{Etch rate} = k_2 \left(\frac{k_1}{k_{-1}}\right)^{1/2} P^{1/2} - \frac{k_2^2}{4 k_{-1}} \qquad (4.10)$$

The mechanism predicts a low pressure first order region and a high pressure half order region, which is observed experimentally. It will be recalled that at high pressures the data was found to fit the equation empirical equation 3.2 :

$$\text{Etch rate} = b(P_{Br_2})^{1/2} - c \qquad (3.2)$$

Comparing this with equation 4.9 :

$$b = k_2 \left(\frac{k_1}{k_{-1}}\right)^{1/2} \qquad (4.11)$$

and :

$$c = \frac{k_2^2}{4k_{-1}} \qquad (4.12)$$

The negative intercept c, is characteristic of half order reactions that result from a dissociative surface adsorption.[53]

It follows from the values obtained for b (section 3.3.2) that :

$$\left(\frac{k_1}{k_{-1}}\right)^{1/2} k_2 = 1.73\ \mu m\ min^{-1}\ Torr^{-1/2}\ e^{(-8.4\,kJ/mol)/RT} \qquad (4.13)$$

where the composite rate constant is the half order rate constant that applies at pressures over approximately 2 Torr.

If the mechanism described by equations 4.1 and 4.2 is correct for the etching of GaAs by molecular bromine, then the reaction occurs by the dissociative adsorption of Br_2 on the GaAs surface. The potential energy barrier for that process is given by the activation energy of k_1, which we find to be 29.2 kJ mol^{-1}.

At high pressures, where reaction (4.1) is reversible the activation energy for the composite half order rate constant gives the height of the potential energy barrier (relative to $Br_2(g)$) for the second step in the reaction. This value is 8.4 kJ mol^{-1}. This information is summarised in the potential energy diagram shown in figure 4.1. The position of the intermediate Br(ads) in the second step and 2Br(ads) in the first step remains undetermined by this data. However, if Br(ads) can be formed directly from bromine atoms in the gas phase, that is :

$$Br(g) \xrightarrow{k_3} Br(ads) \qquad (4.14)$$

then the activation energy for that process fixes the position of Br(ads) on the potential energy diagram. Our experiments yield an

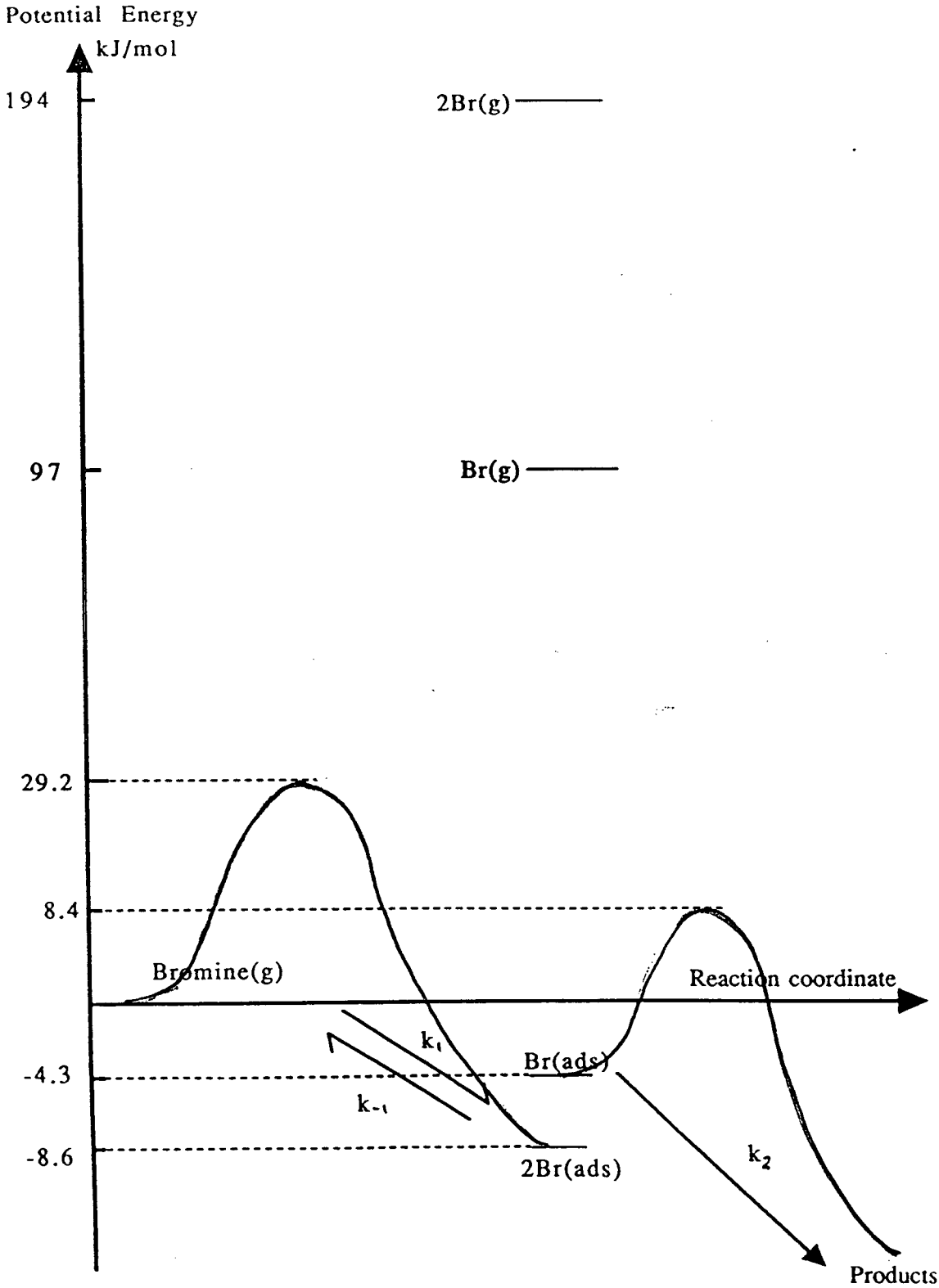

Figure 4.1 Potential energy profile for the bromine and GaAs {100} reaction

activation energy of 12.7 kJ mol^{-1} for that atom reaction, placing Br(ads) at -4.3 kJ and 2Br(ads) at -8.6 kJ.

It is worth noting that because the atomic etching experiments were performed in the low pressure region, where the etch rate is first order with respect to the bromine pressure, the back reaction is slow compared to reaction 4.2. Hence the etch rate is simply given by the sum of the individual etch rates for molecular and atomic etching :

$$\text{Etch rate} = 2k_1[Br_2] + k_3[Br] \qquad (4.15)$$

From the data presented in section 3.4, the Arrhenius plot of the atomic etching experiments yields :

$$k_3 = 1.9 \times 10^5\ \mu m\ min^{-1}\ Torr^{-1}\ e^{(-12.9\ kJ/mol)/RT} \qquad (4.16)$$

The bond energy of bromine is 194 kJ mol^{-1}. The activation energy for the dissociative adsorption of bromine on gallium arsenide which was obtained is only 29.2 kJ mol^{-1}. Much of the energy needed to dissociate the molecule must therefore be provided by the formation of Br(ads)-Ga and Br(ads)-As bonds. From the position of Br(ads) relative to Br(g) in fig. 4.1, these bonds are about 100 kJ mol^{-1}.

The pre-exponential values measured also provide information about the reaction mechanism when compared to the collision frequency. In the low pressure region, the pre-exponential factor A which we have determined for reaction 4.1, is a factor of 10 larger than the collision frequency with the surface. This could be understood if the reaction 4.1 is preceded by pre-adsorption equilibrium described by the equation :

$$Br_2(g) \rightleftharpoons Br_2(ads) \qquad (4.17)$$

Therefore, k_1 is a composite rate constant given by $k_1' K$.

4.3 CONCLUSIONS

The reaction of bromine with GaAs {100} was found to be first order at the lowest pressures used (below 1-2 Torr) and half order at higher pressures. This behaviour is consistent with a mechanism which involves the reversible dissociative adsorption of bromine on a halogenated GaAs surface. This is followed by reaction with the halogenated surface to give the product $AsBr_3$, which desorbs rapidly, and $GaBr_3$ or its dimer Ga_2Br_6, which then probably desorbs more slowly but would not be rate determining under our conditions..

Our results are consistent with the occurrence of at least the following two rate controlling steps :

$$Br_2(g) \underset{k_{-1}}{\overset{k_1}{\rightleftharpoons}} 2Br(ads) \qquad (4.1)$$

$$Br(ads) \xrightarrow{k_2} \text{Products} \qquad (4.2)$$

We find that the rate constant for the first reaction in the forward direction can be represented by the following Arrhenius equation :

$$k_1 = (2.5 \pm 3.2) \times 10^5 \ \mu m \ min^{-1} \ Torr^{-1} \ e^{(-29.2 \pm 4.0 \ kJ/mol)/RT}$$

The composite rate constant and activation energy for the half order reaction are given by

$$\left(\frac{k_1}{k_{-1}}\right)^{1/2} k_2 = 1.73 \pm 0.35 \ \mu m \ min^{-1} \ Torr^{-1/2} \ e^{(-8.4 \pm 0.7 \ kJ/mol)/RT}$$

The rate constant for the reaction with atomic bromine is given by the following Arrhenius equation :

$$k_3 = (1.9 \pm 0.5) \times 10^5 \ \mu m \ min^{-1} \ Torr^{-1} \ e^{(-12.9 \pm 0.9 \ kJ/mol)/RT}$$

References

1 A. D. Milne, MOS Devices : Design and Manufacture, John Wiley and Sons, New York, p1 (1983)

2 P. F. Kane and G. B. Larrabee, Characterisation of Semiconductor Materials, McGraw-Hill Book Company, New York, p2 (1970)

3 J. Millman and A. Grabel, Microelectronics, 2nd Ed., McGraw-Hill Book Company, New York, p8 (1987)

4 G. K. Teal and E. Buehler, Phys Rev., 87, 190 (1952)

5 Y.Tarui, VLSI Technology : Fundamentals and Applications, Springer-Verlag, Berlin, p3 (1986)

6 D. K. Ferry, R. O. Grondin and L. A. Akers, "Two Dimensional Automata in VLSI" in Submicron Integrated Circuits, Editor R. K. Watts, John Wiley and Sons, New York (1989)

7 J. Millman and A. Grabel, Microelectronics, 2nd Ed, McGraw-Hill Book Company, p9 (1987)

8 H. Welker and H. Weiss in Solid State Physics, vol. 3, Editors F. Seitz and D. Turnbull, Academic Press, New York, p1 1956

9 S. K. Ghandhi, VLSI Fabrication Principles : Silicon and Gallium Arsenide, John Wiley and Sons, New York, p12 (1983)

10 J. C. Phillips, Phys. Rev. Lett., 22, 705 (1969)

11 H. C. Gatos and M. C. Lavine, J. Electrochem. Soc., 107, 427 (1960)

12 Y. Tarui, Y. Komiya, Y. Harada, J. Electrochem. Soc., 118, 118 (1971)

13 M. Yokogawa, "LEC GaAs" in Bulk Crystal Growth Technology, editor T. Ikoma, Gordon and Breach Science Publishers, New York (1989)

14 J. W. Mayer and S. S. Lau, Electronics Materials Science : For Integrated Circuits in Si and GaAs, Appendix, Macmillan Publishing Company, New York (1990)

15 Anon, New Scientist, p36, 7th April, 1990

16 M. H. Brodsky, "Progress in Gallium Arsenide Semiconductors", Scientific American, p68, February 1990

17 D. A. Ross, Optoelectronic Devices and Optical Imaging Techniques, Macmillan Press, London, p6 (1979)

18 R. J. Chaffin, Microwave Semiconductor Devices : Fundamentals and Radiation Effects, John Wiley and Sons, New York, p11-14 (1973)

19 F. A. Houle, Basic Mechanisms in Laser Etching and Deposition, Appl. Phys. A41, 315-330 (1986)

20 C. I. H. Ashby, Appl. Phys. Lett., 45, 892 (1984)

21 D. J. Elliot, Integrated Circuit Fabrication Technology, p 359-363, McGraw-Hill Publishing Company (1989)

22 S. K. Ghandhi, VLSI Fabrication Principles : Silicon and Gallium Arsenide, John Wiley and Sons, New York, p499 (1983)

23 J. H. Ha, Ph. D. thesis, Department of Chemistry, U.B.C. (1989)

24 H. F. Winters, J. Appl. Phys., 4, 10 (1978)

25 P. W. Atkins, Physical Chemistry, 3rd Ed., Oxford University Press, Oxford, p772 (1986)

26 Ibid

27 R. P. H. Gasser, An Introduction to Chemisorption and Catalysis by Metals, Oxford University Press, Oxford, p177 (1985)

28 J. E. Lennard-Jones, Trans. Farad. Soc., 28, 333 (1932)

29 J. M. Thomas and W. J. Thomas, Introduction to the Principles of Heterogeneous Catalysis, Academic Press, London (1967)

30 D. L. Flamm, V. M. Donnelly and D. E. Ibbotson, J. Vac. Sci. Technol. B1(1), 23 (1983)

31 I. Langmuir, Trans. Farad. Soc., 17, 607 (1922)

32 J. F. Lynch and T. B. Flanagan, J. Phys. Chem., 77, 2628 (1973)

33 R. H. Burton, R. A. Gottscho and G. Smolinsky, "Dry Etching of Group III-V Compound Semiconductors" in Dry Etching for Microelectronics, Editor R. A. Powell, Elsevier Science Publishers (1984)

34 V. M. Donnelly, D. L. Flamm and D. E. Ibbotson, J. Vac. Sci. Technol. A 1, 626 (1983)

35 G. Smolinsky, R. P. Chang and T. M. Mayer, J. Vac. Sci. Technol., 18, 12 (1981)

36 D. E. Ibbotson, D. L. Flamm and V. M. Donnelly, J. Appl. Phys., 54, 5974 (1983)

37 V. M. Donnelly, D. L. Flamm, C. W. Tu and D. E. Ibbotson, J. Electrochem. Soc., 129, 5974 (1983)

38 J. H. Ha, Ph. D. Thesis, Department of Chemistry, U.B.C. (1989)

39 J. H. Ha, E. A. Ogryzlo and S. Polyhronopoulos, J. Chem. Phys., 89, (5), 2844 (1988)

40 N. Furuhata, H. Miyamoto, A. Okamoto and K. Ohata, J. Elect. Mat., 19, 201 (1990)

41 M. Balooch and D. R. Olander, J. Vac. Sci. Technol. B 4, 794 (1986)

42 K. R. Jennings, Quart. Rev., 15, 237 (1961)

43 E. A. Ogryzlo, Can. J. Chem., 39, 2556 (1961)

44 L. Elias, E. A. Ogryzlo and H. I. Schiff, Can. J. Chem., 37, 1680 (1959)

45 R. C. Weast, CRC Handbook of Chemistry and Physics, 61st Ed., F-222 (1980-1981)

46 Z. H. Walker, unpublished results.

47 D. C. Chong, unpublished results

48 R. H. Williams and I. T. McGovern, "Adsorption on Semiconductors" in The Chemical Physics of Solid Surfaces and Heterogeneous Catalysis, Editors D. A. King and D. P. Woodruff, vol. 3, p298, Elsevier Science Publishers, Amsterdam (1984)

49 Bromine and its Compounds, Ed. Z. E. Jolles, Academic Press, New York, p222 (1966)

50 Ibid, p131

51 K. Wade and A. J. Bannister, "Aluminium, gallium, indium and thallium" in Comprehensive Inorganic Chemistry, vol. 1, Executive editor A. F. Trotman-Dickenson, Pergamon Press, London, p993 (1973)

52 V. M. Donnelly, D. L. Flamm, C. W. Tu and D. E. Ibbotson, J. Vac. Sci. Technol. B 4, 794 (1986)

53 C. J. Smithells, C. E. Ransley, Roy. Soc. Proc. A, 150, 172 (1935)